A Direct Comparison of the Rates of Degenerate Transfer of Electrons, Protons, and Hydrogen Atoms between Metal Complexes†

John D. Protasiewicz and Klaus H. Theopold*

Contribution from the Department of Chemistry and Biochemistry, Center for Catalytic Science and Technology, University of Delaware, Newark, Delaware 19716

Received September 4, 1992

Abstract: Tp*Mo(CO)$_3$H (Tp* = hydridotris(3,5-dimethylpyrazolyl)borate) crystallized in the monoclinic space group $P2_1/c$ with a = 8.005(3) Å, b = 13.873(5) Å, c = 18.874(5) Å, β = 97.73(2)°, and Z = 4. Oxidation of Et_4N[Tp*Mo(CO)$_3$] with [Cp_2Fe]PF_6 yielded Tp*Mo(CO)$_3$; this 17-electron radical also crystallized in the monoclinic space group $P2_1/c$ with a = 7.962(4) Å, b = 13.885(6) Å, c = 19.048(5) Å, β = 96.86(2)°, and Z = 4. The pK_a of TpMo(CO)$_3$H (Tp = hydridotris(pyrazolyl)borate) in acetonitrile was 11.3(2) and D_{Mo-H} measured 63(1) kcal/mol. Equilibration of TpMo(CO)$_3$H with Tp*Mo(CO)$_3$ afforded the corresponding values for Tp*Mo(CO)$_3$H: D_{Mo-H} = 60(1) kcal/mol and pK_a = 10.2. The rates of degenerate electron transfer between ^{n}Bu$_4$N[Tp*Mo(CO)$_3$] and Tp*Mo(CO)$_3$ in THF were measured by ^{1}H NMR line broadening: k_2(30 °C) = 8.6 × 10^6 M^{-1} s^{-1}, ΔH^* = 3.5(2) kcal/mol, ΔS^* = −15.3(6) cal/(mol·K). The rates of degenerate proton transfer between Tp*Mo(CO)$_3$H and ^{n}Bu$_4$N[Tp*Mo(CO)$_3$] in THF were measured by a selective inversion recovery NMR experiment and by ^{1}H NMR monitoring of the reaction of deuterium-labeled (Tp*-d$_4$)Mo(CO)$_3$H with ^{n}Bu$_4$N[Tp*Mo(CO)$_3$]: k_2(30 °C) = 3.5 M^{-1} s^{-1}, ΔH^* = 3.6(2) kcal/mol, ΔS^* = −45(1) cal/(mol·K). The proton transfer was catalyzed by bromide and chloride ions. The rates of degenerate hydrogen atom transfer were measured by monitoring the reaction of Tp*Mo(CO)$_3$H with Tp*Mo(^{13}CO)$_3$ in THF at −34 °C by ^{13}C NMR. The hydrogen atom transfer was catalyzed by both base and acid. The slowest rate constant measured (k_2(−34 °C) = 9.0 × 10^{-3} M^{-1} s^{-1}) established an upper limit for the rate of hydrogen atom transfer. In this particular system electron transfer is very fast, proton transfer is slow, and hydrogen atom transfer is slower yet.

Introduction

Among the elementary reaction steps of catalytic cycles one often encounters electron transfers and atom transfer reactions (e.g. H$^+$, H$^•$, H$^-$, O, etc.).[1] The rates and mechanisms of redox processes involving coordination compounds have been studied for some time, and Marcus theory is firmly entrenched as the theoretical basis for the interpretation of such measurements[2] (note however the paucity of data for organometallic complexes). Much less is known about the factors that control the rates of atom transfer processes between metal complexes.

There are obvious parallels between the transfer of the lightest of all nuclei and that of electrons, and Marcus and others have discussed these.[3] Attempts have indeed been made to extend the Marcus treatment to group transfer reactions involving entities as large as alkyl groups.[4] Whereas such broad applicability of the theory would be intellectually satisfying, experimental data are needed to test this notion. Furthermore, it should be informative to directly compare electron and hydrogen transfer rates and mechanisms within the same set of compounds. Such a direct comparison was the object of the research described herein. More specifically, we set out to measure rates of hydrogen atom transfer, proton transfer, and electron transfer between the same metal complexes.

The transfer of hydrogen atoms (H$^•$) between metal complexes is a reaction with some precedent.[5] However, this quintessential 1-electron transformation violates one of the most basic rules of organometallic chemistry, which states that "organometallic reactions, including catalytic ones, proceed by elementary steps involving only intermediates with 16 or 18 metal valence electrons".[6] Clearly, some of the reactants as well as the products of hydrogen atom transfer will have odd electron counts. Such species are commonly unstable with respect to further reaction (e.g. disproportionation, ligand substitution, or dimerization), and for this reason the reaction of interest here (i.e. H$^•$ transfer) can rarely be observed and studied directly. Much more often the hydrogen atom transfer constitutes only one step in a radical chain reaction. Thus very few rate measurements are available. For some notable exceptions see eqs 1–4. On the basis of these numbers and kinetic requirements of radical chain reactions, H$^•$

† Dedicated to Prof. R. A. Marcus on the occasion of his being awarded the 1992 Nobel Prize in Chemistry.

(1) (a) Kochi, J. K. *Organometallic Mechanisms and Catalysis*; Academic Press: New York, 1978. (b) Halpern, J. *Pure Appl. Chem.* **1979**, *51*, 2171. (c) Bullock, M. *Comments Inorg. Chem.* **1991**, *12*, 1. (d) Eisenberg, D. C.; Norton, J. R. *Isr. J. Chem.* **1991**, *31*, 55. (e) Holm, R. H. *Chem. Rev.* **1987**, *87*, 1401.

(2) (a) Marcus, R. A. *J. Chem. Phys.* **1956**, *24*, 966. (b) Marcus, R. A.; Sutin, N. *Biochim. Biophys. Acta* **1985**, *811*, 265. (c) Lippard, S. J., Ed. *Prog. Inorg. Chem.* **1983**, *30*.

(3) (a) Marcus, R. A. *J. Phys. Chem.* **1968**, *72*, 891. (b) Dogonadze, R. R.; Kuznetzov, A. M.; Levich, V. G. *Electrochim. Acta* **1968**, *13*, 1025. (c) Kato, S.; Kato, H.; Fukui, K. *J. Am. Chem. Soc.* **1977**, *99*, 684. (d) Brünische-Olsen, N.; Ulstrup, J. *J. Chem. Soc., Faraday Trans.* **1979**, *75*, 205. (e) German, E. D.; Kuznetzov, A. M.; Dogonadze, R. R. *J. Chem. Soc., Faraday Trans.* **1980**, 1128. (f) Trakhtenberg, L. I.; Klochikin, V. L.; Pshezhetsky, S. Ya. *Chem. Phys.* **1982**, *69*, 121. (g) Warshel, A. *J. Phys. Chem.* **1982**, *86*, 2218. (h) Marcus, R. A. In *Proceedings of the Symposium on the Chemistry and Physics of Electroanalysis* (1983, San Francisco, CA); McIntyre, J. D. E., Weaver, M. J., Yeager, E. B., Eds.; Pennington: New Jersey, 1984; pp 169–186. (i) Siebrand, W.; Wildman, T. A.; Zgierski, M. Z. *J. Am. Chem. Soc.* **1984**, *106*, 4083. (j) Meyer, R.; Ernst, R. R. *J. Chem. Phys.* **1987**, *86*, 784. (k) Creutz, C.; Sutin, N. *J. Am. Chem. Soc.* **1988**, *110*, 2418. (l) Borgis, D. C.; Lee, S.; Hynes, J. T. *Chem. Phys. Lett.* **1989**, *162*, 19. (m) Kristjansdottir, S. S.; Norton, J. R. *J. Am. Chem. Soc.* **1991**, *113*, 4366. (n) Choi, M.-G.; Brown, T. L. *Inorg. Chim. Acta* **1992**, *198–200*, 823.

(4) (a) Albery, W. J. *Annu. Rev. Phys. Chem.* **1980**, *31*, 227. (b) Wang, P.; Atwood, J. D. *J. Am. Chem. Soc.* **1992**, *114*, 6424.

(5) (a) Byers, B. H.; Brown, T. L. *J. Am. Chem. Soc.* **1977**, *99*, 2527. (b) Hoffman, W. N.; Brown, T. L. *Inorg. Chem.* **1978**, *17*, 613. (c) Sumner, C. E.; Nelson, G. E. *J. Am. Chem. Soc.* **1984**, *106*, 432. (d) Narayanan, B. A.; Amatore, C. A.; Casey, C. P.; Kochi, J. K. *J. Am. Chem. Soc.* **1983**, *105*, 6351. (e) McCullen, S. B.; Brown, T. L. *J. Am. Chem. Soc.* **1982**, *104*, 7496. (f) Walker, H. W.; Rattinger, G. B.; Belford, R. L.; Brown, T. L. *Organometallics* **1983**, *2*, 775. (g) Lapinte, C.; Catheline, D.; Astruc, D. *Organometallics* **1984**, *3*, 817. (h) Nappa, M. J.; Santi, R.; Halpern, J. *Organometallics* **1985**, *4*, 34. (i) Cooley, N. A.; Watson, K. A.; Fortier, S.; Baird, M. C. *Organometallics* **1986**, *5*, 2563. (j) Song, J.-S.; Bullock, R. M.; Creutz, C. *J. Am. Chem. Soc.* **1991**, *113*, 9862.

(6) Tolman, C. A. *Chem. Soc. Rev.* **1972**, *1*, 337.

0002-7863/93/1515-5559$04.00/0

transfer is generally thought to be very fast.

$$Mn(CO)_3(P^nBu_3)_2 + HSn^nBu_3 \rightarrow HMn(CO)_3(P^nBu_3)_2 + {}^1/_2Sn_2{}^nBu_3 \quad (1)$$

$k = 10.7\ M^{-1}\ s^{-1}$ (at 20 °C in hexane)[5e]

$$*[Pt_2(P_2O_5H_2)_4]^{4-} + HSnPh_3 \rightarrow [HPt_2(P_2O_5H_2)_4]^{4-} + SnPh_3 \quad (2)$$

$k = 1.0 \times 10^8\ M^{-1}\ s^{-1}$ (at 25 °C in acetonitrile)[7]

$$CpCr(CO)_3 + CpCr(CO)_3H \rightleftharpoons CpCr(CO)_3H + CpCr(CO)_3 \quad (3)$$

$k > 10^3\ M^{-1}\ s^{-1}$

(fast on ^1H NMR time scale at room temperature)[5i]

$$Cp^DW(CO)_3 + CpW(CO)_3H \rightleftharpoons Cp^DW(CO)_3H + CpW(CO)_3 \quad (4)$$

$k > 10^6\ M^{-1}\ s^{-1}$ (at 25 °C in acetonitrile, $Cp^D = \eta^5$-C_5D_5)[5j]

A good deal more is known about proton (H^+) transfer rates between metal complexes, primarily due to the work of Norton et al.[8] These acid/base reactions are relatively slow (typical rate constants for the deprotonation of an organometallic acid by its conjugate base fall in the range 10^{-1}–$10^{-5}\ M^{-1}\ s^{-1}$), resembling in this respect proton transfers to and from carbon.[9]

For the purposes of this study we were looking for triads of compounds, consisting of a metal hydride (HML_n), its conjugate base ($[ML_n]^-$), and the one-electron oxidation product of the latter ($^\bullet ML_n$), all stable and isolable. Under these circumstances the three possible combinations of two of the above reagents set up degenerate exchange reactions involving—at least formally—the transfer of electrons (eq 5), protons (eq 6), and hydrogen atoms (eq 7). Measurement of the degenerate exchange rates would then allow a comparison of intrinsic barriers of reactions, which are as nearly comparable as possible.

$$[MN_n]^- + {}^\bullet ML_n \rightleftharpoons {}^\bullet ML_n + [ML_n]^- \quad (5)$$

$$HML_n + [ML_n]^- \rightleftharpoons [ML_n]^- + HML_n \quad (6)$$

$$HML_n + {}^\bullet ML_n \rightleftharpoons {}^\bullet ML_n + HML_n \quad (7)$$

The first set of compounds we chose for our investigation consisted of the cobalt phosphite complexes $HCo[P(OMe)_3]_4$, $KCo[P(OMe)_3]_4$, and $Co[P(OMe)_3]_4$, all previously prepared by Muetterties et al.[10] Having measured the rate of electron transfer for this system ($k_{et}(294K) = 8.8 \times 10^3\ M^{-1}\ s^{-1}$),[11] we found, however, that both proton and hydrogen atom transfer were immeasurably slow ($k_2 < 10^{-6}\ M^{-1}\ s^{-1}$), even at elevated temperatures. On the basis of the interpretation that excessive steric hindrance was responsible for this observation, we turned to a set of metal carbonyls, namely $Tp^*Mo(CO)_3H$, $NR_4[Tp^*Mo(CO)_3]$, and $Tp^*Mo(CO)_3$ (Tp^* = hydridotris(3,5-dimethylpyrazolyl)borate). While the Tp^* ligand is bulky enough to prevent dimerization of the 17-electron complex $Tp^*Mo(CO)_3$, the open carbonyl side of the complexes was thought to allow for closer M···H···M interactions, thereby facilitating exchange. The following is a detailed account of our study of the latter system.

Results and Discussion

Synthesis. The hydrides $Tp^*Mo(CO)_3H$ and $TpMo(CO)_3H$ (Tp = hydridotris(pyrazolyl)borate) as well as salts of the carbonylate anions $[Tp^*Mo(CO)_3]^-$ and $[TpMo(CO)_3]^-$ were originally prepared by Trofimenko.[12] Seeking to circumvent the thermal instability of the radical $TpMo(CO)_3$—characterized earlier by Curtis et al.[13]—we began by preparing the analogous $Tp^*Mo(CO)_3$. While this work was in progress Shiu et al. reported the synthesis of this robust metalaradical.[14]

We have found that $Tp^*Mo(CO)_3H$ was conveniently prepared by protonation of $Et_4N[Tp^*Mo(CO)_3]$ with $HBF_4{\cdot}Et_2O$ in acetonitrile. The hydride was insoluble in this solvent and precipitated as a yellow microcrystalline solid. Solutions of $Tp^*Mo(CO)_3H$ in CD_2Cl_2 exhibited the characteristic hydride resonance at δ −3.41 ppm in the ^1H NMR spectrum. In order to facilitate identification of the M–H stretching vibration, $Tp^*Mo(CO)_3D$ was prepared by exchange with D_2O. Interestingly, the differences in the IR spectra (see supplementary material) of the two isotopomers were confined to the carbonyl stretching region. The solid-state IR spectrum (KBr pellet) of $Tp^*Mo(CO)_3H$ exhibited a sharp band at 1998 cm^{-1} as well as a broader feature consisting of four resolved bands at 1914, 1900, 1889, and 1870 cm^{-1}. The corresponding spectrum of $Tp^*Mo(CO)_3D$ featured a sharp resonance at 2000 cm^{-1} and a broad feature with only two apparent peaks at 1901 and 1880 cm^{-1}. There were no significant differences in the other regions of the spectra. As no more than four modes (3 ν_{CO} and 1 ν_{MH}) are expected in this region for isolated $Tp^*Mo(CO)_3H$, solid-state effects must be responsible for the further splitting. However, the difference in the solid-state spectra of hydride and deuteride pointed toward a contribution from M–H(D) vibrations. To avoid the symmetry lowering of the crystalline environment, solution spectra (in THF) were recorded. While the solution spectrum of $Tp^*Mo(CO)_3D$ exhibited three symmetric bands at 2000, 1912, and 1886 cm^{-1}, the hydride spectrum clearly showed a shoulder on the resonance of lowest energy (i.e. bands at 2000, 1913, and 1893 cm^{-1} with a shoulder at ca. 1880 cm^{-1}). These observation are consistent with a Fermi resonance interaction between ν_{MH} (approximately at 1886 cm^{-1}, but lowered by the mixing) and one of the carbonyl stretches.[15] A possible explanation for the absence of any observable ν_{MD} involves "intensity stealing" connected with the Fermi resonance, benefiting only ν_{MH} of an inherently weak M–H(D) vibration.

For the purposes of the exchange studies (see below) we have also prepared $(Tp^*\text{-}d_4)Mo(CO)_3H$, a labeled derivative of $Tp^*Mo(CO)_3H$ with deuterium atoms in the C4-positions of all three pyrazole rings as well as on the boron. Curiously, $(Tp^*\text{-}d_4)Mo(CO)_3H$ was found to react with strong acids, resulting in loss of deuterium label from the pyrazole rings. Thus reaction with trichloroacetic acid in CD_2Cl_2 resulted in slow exchange (half-life of ca. 1 h, monitored by ^1H NMR). The exchange between $(Tp^*\text{-}d_4)Mo(CO)_3H$ and trifluoroacetic acid reached equilibrium before an NMR spectrum could be recorded. As $Tp^*Mo(CO)_3H$ is a moderately strong acid itself, one might expect scrambling of the label in pure $(Tp^*\text{-}d_4)Mo(CO)_3H$; indeed, when a THF-$d_8$ solution of it was heated to 75 °C for several days, the signal intensity of the C4-proton increased at the cost of a

(7) (a) Vlcek, A.; Gray, H. B. *J. Am. Chem. Soc.* **1987**, *109*, 286. (d) Vlcek, A.; Gray, H. B. *Inorg. Chem.* **1987**, *26*, 1997.

(8) (a) Jordan, R. F.; Norton, J. R. *J. Am. Chem. Soc.* **1982**, *104*, 1255. (b) Jordan, R. F.; Norton, J. R. *ACS Symp. Ser.* **1982**, *No. 198*, 403. (c) Moore, E. J.; Sullivan, J. M.; Norton, J. R. *J. Am. Chem. Soc.* **1986**, *108*, 2257. (d) Edidin, R. T.; Sullivan, J. M.; Norton, J. R. *J. Am. Chem. Soc.* **1987**, *109*, 3945. (e) Kristjansdottir, S. S.; Moody, A. E.; Weberg, R. T.; Norton, J. R. *Organometallics* **1988**, *7*, 1983. (f) Weberg, R. T.; Norton, J. R. *J. Am. Chem. Soc.* **1990**, *112*, 1105.

(9) Kresge, A. J. *Acc. Chem. Res.* **1975**, *8*, 354.

(10) (a) Muetterties, E. L.; Bleeke, J. R.; Yang, Z.-Y.; Day, V. W. *J. Am. Chem. Soc.* **1982**, *104*, 2940. (b) Muetterties, E. L.; Hirsekorn, F. J. *J. Am. Chem. Soc.* **1974**, *96*, 7920.

(11) Protasiewicz, J. D.; Schulte, G.; Theopold, K. H. *Inorg. Chem.* **1988**, *27*, 1133.

(12) (a) Trofimenko, S. *J. Am. Chem. Soc.* **1969**, *91*, 588. (b) Trofimenko, S. *J. Am. Chem. Soc.* **1967**, *89*, 6288.

(13) (a) Shiu, K.-B.; Curtis, M. D.; Huffman, J. C. *Organometallics* **1982**, *2*, 936. (b) Curtis, M. D.; Shiu, K. B.; Butler, W. M.; Huffman, J. C. *J. Am. Chem. Soc.* **1986**, *108*, 3335.

(14) Shiu, K.-B.; Lee, L.-Y. *J. Orgmet. Chem.* **1988**, *348*, 357.

(15) (a) Kaesz, H. D.; Saillant, R. B. *Chem. Rev.* **1972**, *72*, 231. (b) Ebsworth, E. A. V.; Rankin, D. W. H.; Cradock, S. *Structural Methods in Inorganic Chemistry*, 2nd ed.; CRC Press: Boca Raton, FL, 1991; pp 173–254.

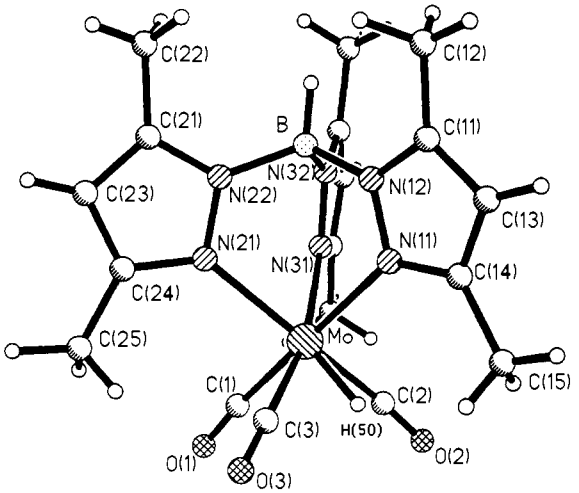

Figure 1. Molecular structure of $Tp^*Mo(CO)_3H$. Interatomic distances and angles are listed in Table I.

diminishing hydride signal. At the same time increasing resonances attributable to $Tp^*Mo(CO)_3$ signaled the onset of thermal decomposition of the hydride.

Oxidation of $Et_4N[Tp^*Mo(CO)_3]$ with $[Cp_2Fe]PF_6$, as described by Shiu et al.,[14] yielded paramagnetic $Tp^*Mo(CO)_3$ in essentially quantitative yield. Its IR spectrum (KBr) showed the expected two CO stretches of a tricarbonyl moiety with C_{3v} symmetry (1997, 1851 cm^{-1}) and the ^1H NMR spectrum featured relatively sharp but shifted resonances (THF-d_8, 22 °C: δ 36.2 (9H), 18.3 (9H), 10.6 (br, 1H), 1.38 (3H) ppm). As expected, the latter exhibited linear dependencies on $1/T$. The magnetic susceptibility of solid $Tp^*Mo(CO)_3$ was measured with a Faraday balance in the temperature interval 153–292 K. The data were fitted with a Curie–Weiss expression;[16] the effective magnetic moment at room temperature (μ_{eff}(292K) = 2.13 μ_B) was consistent with the presence of one unpaired electron. $Tp^*Mo(CO)_3$ is very stable; it does not decompose upon heating to 100 °C in solution and may be sublimed in vacuo at 150 °C.

The acid lability of the deuterium label in $(Tp^*\text{-}d_4)Mo(CO)_3H$ necessitated the preparation of a complex with a different label. Thus $Tp^*Mo(^{13}CO)_3$ was prepared by repeated equilibration of $Tp^*Mo(CO)_3$ with excess ^{13}CO at 100 °C (exchange proved too slow at 80 °C!). The IR spectrum of $Tp^*Mo(^{13}CO)_3$ so obtained (KBr: 1950, 1811 cm^{-1}) revealed no remaining ^{12}CO. However, the extent of ^{13}CO incorporation was best determined by conversion to $Tp^*Mo(^{13}CO)_3H$ and analysis by ^1H NMR. By this method (see Experimental Section) it was determined that 94% of all bound carbon monoxide was ^{13}CO, distributed over $Tp^*Mo(^{13}CO)_3$ (82%), $Tp^*Mo(^{13}CO)_2(^{12}CO)$ (16%), and $Tp^*Mo(^{13}CO)(^{12}CO)_2$ (2%).

The complete insolubility of $Et_4N[Tp^*Mo(CO)_3]$ in CH_2Cl_2 or THF was overcome by preparation of $^nBu_4N[Tp^*Mo(CO)_3]$, which is soluble even in toluene. The solution IR spectra of this salt in a variety of solvents (toluene, dichloromethane, acetonitrile) all showed two bands, providing no apparent evidence for strong ion pairing.

Structure Determinations. As the basis for interpretation of rates of the degenerate exchange reactions, complete structural characterization of the three complexes used in this study was desirable. The crystal structure of $Et_4N[Tp^*Mo(CO)_3]$ has been reported.[17] We have therefore determined the structures of $Tp^*Mo(CO)_3H$ and $Tp^*Mo(CO)_3$ by X-ray diffraction.

A single crystal of $Tp^*Mo(CO)_3H$ was grown by vapor diffusion of pentane into a saturated solution of the hydride in dichloromethane. Data collection was carried out at −75 °C. The result of the structure determination is shown in Figure 1; interatomic distances and angles are listed in Table I. The crystal belongs to the space group $P2_1/c$; individual molecules contain no crystallographic symmetry elements. The molybdenum is 7-coordinate. Three adjacent coordination sites are taken up by N atoms of the Tp* ligand with an average Mo–N distance of 2.237 Å. Bond distances and angles within the Tp* ligand are normal. The three carbonyl ligands are coordinated approximately trans to the pyrazole nitrogens. However, one of the C–Mo–C angles is larger (103°) than the other two (79, 82°) by ca. 20°, thereby making room for the hydride ligand. The latter was located in a difference map and its position was refined. The Mo–H distance of 1.44 Å is shorter than previously determined values for molybdenum hydrides (1.59–1.82 Å),[18] but hydrogen positions determined by X-ray diffraction must of course be viewed with some caution. $Tp^*Mo(CO)_3H$ is closely related structurally to the tungsten analogue $Tp^*W(CO)_3H$, the structure of which has recently been reported.[19]

Table I. Interatomic Distances (Å) and Angles (deg) for $Tp^*Mo(CO)_3H$

atoms	distance[a]	atoms	distance[a]
Mo–H(50)	1.436	Mo–N(11)	2.252(2)
Mo–N(21)	2.230(2)	Mo–N(31)	2.230(2)
Mo–C(1)	1.977(3)	Mo–C(2)	1.974(3)
Mo–C(3)	1.987(3)	N(11)–N(12)	1.367(3)
N(11)–C(14)	1.352(3)	N(12)–B	1.537(4)
N(12)–C(11)	1.352(4)	N(21)–N(22)	1.379(3)
N(21)–C(24)	1.352(4)	N(22)–B	1.543(4)
N(22)–C(21)	1.347(4)	N(31)–N(32)	1.383(3)
N(31)–C(34)	1.350(4)	N(32)–B	1.550(4)
N(32)–C(31)	1.348(4)	O(1)–C(1)	1.153(4)
O(2)–C(2)	1.153(4)	O(3)–C(3)	1.148(4)
B–H(40)	1.034	C(11)–C(12)	1.496(4)
C(11)–C(13)	1.380(4)	C(13)–C(14)	1.389(4)
C(14)–C(15)	1.496(4)	C(21)–C(22)	1.492(4)
C(21)–C(23)	1.374(5)	C(23)–C(24)	1.382(4)
C(24)–C(25)	1.482(5)	C(31)–C(32)	1.495(4)
C(31)–C(33)	1.379(4)	C(33)–C(34)	1.394(4)
C(34)–C(35)	1.498(4)		

atoms	angle[a]	atoms	angle[a]
H(50)–Mo–N(11)	81.4(1)	H(50)–Mo–N(21)	140.2(1)
N(11)–Mo–N(21)	85.7(1)	H(50)–Mo–N(31)	134.5(1)
N(11)–Mo–N(31)	81.8(1)	N(21)–Mo–N(31)	79.8(1)
H(50)–Mo–C(1)	99.0(1)	N(11)–Mo–C(1)	179.0(1)
N(21)–Mo–C(1)	94.6(1)	N(31)–Mo–C(1)	97.3(1)
H(50)–Mo–C(2)	52.4(1)	N(11)–Mo–C(2)	100.6(1)
N(21)–Mo–C(2)	197.2(1)	N(31)–Mo–C(2)	90.1(1)
C(1)–Mo–C(2)	78.9(1)	H(50)–Mo–C(3)	58.5(1)
N(11)–Mo–C(3)	98.9(1)	N(21)–Mo–C(3)	86.9(1)
N(31)–Mo–C(3)	166.6(1)	C(1)–Mo–C(3)	82.1(1)
C(2)–Mo–C(3)	102.9(1)	Mo–N(11)–N(12)	119.7(2)
Mo–N(11)–C(14)	133.2(2)	N(12)–N(11)–C(14)	106.6(2)
N(11)–N(12)–B	119.5(2)	N(11)–N(12)–C(11)	110.1(2)
B–N(12)–C(11)	130.0(2)	Mo–N(21)–N(22)	119.9(2)
Mo–N(21)–C(24)	133.8(2)	N(22)–N(21)–C(24)	106.2(2)
N(21)–N(22)–B	120.1(2)	N(21)–N(22)–C(21)	109.8(2)
B–N(22)–C(21)	130.0(2)	Mo–N(31)–N(32)	119.0(2)
Mo–N(31)–C(34)	134.6(2)	N(32)–N(31)–C(34)	106.2(2)
N(31)–N(32)–B	120.4(2)	N(31)–N(32)–C(31)	109.8(2)
B–N(32)–C(31)	129.4(2)	N(12)–B–N(22)	109.6(2)
N(12)–B–N(32)	109.4(2)	N(22)–B–N(32)	108.4(2)
Mo–C(1)–O(1)	174.6(2)	Mo–C(2)–O(2)	175.8(3)
Mo–C(3)–O(3)	179.8(4)	N(12)–C(11)–C(12)	123.7(3)
N(12)–C(11)–C(13)	107.4(2)	C(12)–C(11)–C(13)	128.9(3)
C(11)–C(13)–C(14)	106.5(2)	N(11)–C(14)–C(13)	109.3(2)
N(11)–C(14)–C(15)	123.1(3)	C(13)–C(14)–C(15)	127.6(3)
N(22)–C(21)–C(22)	122.5(3)	N(22)–C(21)–C(23)	107.6(3)
C(22)–C(21)–C(23)	129.8(3)	C(21)–C(23)–C(24)	107.0(3)
N(21)–C(24)–C(23)	109.3(3)	N(21)–C(24)–C(25)	124.0(3)
C(23)–C(24)–C(25)	126.7(3)	N(32)–C(31)–C(32)	123.5(2)
N(32)–C(31)–C(33)	108.1(2)	C(32)–C(31)–C(33)	128.5(3)
C(31)–C(33)–C(34)	106.2(3)	N(31)–C(34)–C(33)	109.7(2)
N(31)–C(34)–C(35)	122.9(3)	C(33)–C(34)–C(35)	127.4(3)

[a] Estimated standard deviations are given in parentheses.

(16) Carlin, R. L. *Magnetochemistry*; Springer: Berlin, 1986; p 14. Curie-Weiss expression: $\chi_m = [C/(T-\theta)]$; C = 0.415 emu·K/mol, θ = 16.5 K.

(17) Marabella, C. P.; Enemark, J. H. *J. Organomet. Chem.* **1982**, *226*, 57.

(18) Teller, R. G.; Bau, R. In *Structure Bonding* **1981**, *44*, 1.

Table II. Interatomic Distances (Å) and Angles (deg) for $Tp^*Mo(CO)_3$

atoms	distance[a]	atoms	distance[a]
Mo–N(11)	2.225(3)	Mo–N(21)	2.205(3)
Mo–N(31)	2.196(3)	Mo–C(1)	1.971(4)
Mo–C(2)	1.984(3)	Mo–C(3)	2.018(4)
N(11)–N(12)	1.378(3)	N(11)–C(14)	1.342(4)
N(12)–B	1.544(4)	N(12)–C(11)	1.345(4)
N(21)–N(22)	1.378(4)	N(21)–C(24)	1.351(4)
N(22)–B	1.546(5)	N(22)–C(21)	1.351(4)
N(31)–N(32)	1.388(3)	N(31)–C(34)	1.343(4)
N(32)–B	1.545(4)	N(32)–C(31)	1.351(4)
O(1)–C(1)	1.158(5)	O(2)–C(2)	1.157(4)
O(3)–C(3)	1.150(4)	C(11)–C(12)	1.499(5)
C(11)–C(13)	1.384(4)	C(13)–C(14)	1.387(5)
C(14)–C(15)	1.496(4)	C(21)–C(22)	1.484(5)
C(21)–C(23)	1.379(5)	C(23)–C(24)	1.388(5)
C(24)–C(25)	1.490(5)	C(312)–C(32)	1.495(5)
C(31)–C(33)	1.377(4)	C(33)–C(34)	1.386(5)
C(34)–C(35)	1.496(5)		

atoms	angle[a]	atoms	angle[a]
N(11)–Mo–N(21)	85.6(1)	N(11)–Mo–N(31)	83.0(1)
N(21)–Mo–N(31)	82.1(1)	N(11)–Mo–C(1)	175.5(1)
N(21)–Mo–C(1)	98.4(1)	N(31)–Mo–C(1)	99.6(1)
N(11)–Mo–C(2)	97.9(1)	N(21)–Mo–C(2)	174.3(1)
N(31)–Mo–C(2)	93.8(1)	C(1)–Mo–C(2)	78.4(1)
N(11)–Mo–C(3)	93.9(1)	N(21)–Mo–C(3)	90.9(1)
N(31)–Mo–C(3)	172.6(1)	C(1)–Mo–C(3)	83.9(1)
C(2)–Mo–C(3)	93.3(1)	Mo–N(11)–N(12)	119.5(2)
Mo–N(11)–C(14)	133.7(2)	N(12)–N(11)–C(14)	106.4(2)
N(11)–N(12)–B	118.9(2)	N(11)–N(12)–C(11)	109.9(2)
B–N(12)–C(11)	131.0(3)	Mo–N(21)–N(22)	119.9(2)
Mo–N(21)–C(24)	133.8(2)	N(22)–N(21)–C(24)	106.3(2)
N(21)–N(22)–B	119.5(2)	N(21)–N(22)–C(21)	110.0(2)
B–N(22)–C(21)	130.4(2)	Mo–N(31)–N(32)	118.3(2)
Mo–N(31)–C(34)	135.0(2)	N(32)–N(31)–C(34)	106.6(2)
N(31)–N(32)–B	121.0(2)	N(31)–N(32)–C(31)	109.0(2)
B–N(32)–C(31)	129.9(3)	N(12)–B–N(22)	109.4(2)
N(12)–B–N(32)	109.4(2)	N(22)–B–N(32)	108.8(2)
Mo–C(1)–O(1)	172.9(3)	Mo–C(2)–O(2)	174.1(3)
Mo–C(3)–O(3)	177.3(3)	N(12)–C(11)–C(12)	123.4(3)
N(12)–C(11)–C(13)	107.6(3)	C(12)–C(11)–C(13)	129.1(3)
C(11)–C(13)–C(14)	106.2(3)	N(11)–C(14)–C(13)	109.9(3)
N(11)–C(14)–C(15)	121.5(3)	C(13)–C(14)–C(15)	128.6(3)
N(22)–C(21)–C(22)	122.8(3)	N(22)–C(21)–C(23)	107.5(3)
C(22)–C(21)–C(23)	129.7(3)	C(21)–C(23)–C(24)	106.7(3)
N(21)–C(24)–C(23)	109.5(3)	N(21)–C(24)–C(25)	122.8(3)
C(23)–C(24)–C(25)	127.7(3)	N(32)–C(31)–C(32)	123.0(3)
N(32)–C(31)–C(33)	108.2(3)	C(32)–C(31)–C(33)	128.8(3)
C(31)–C(33)–C(34)	106.4(3)	N(31)–C(34)–C(33)	109.8(3)
N(31)–C(34)–C(35)	122.5(3)	C(33)–C(34)–C(35)	127.7(3)

[a] Estimated standard deviations are given in parentheses.

A crystal of $Tp^*Mo(CO)_3$ was grown by the same technique, and the data collection was once again carried out at −75 °C. The molecular structure of the radical is depicted in Figure 2; the corresponding distances and angles are collected in Table II. This crystal also belonged to the space group $P2_1/c$; furthermore, the unit cell parameters differed by less than 1% from those of $Tp^*Mo(CO)_3H$. However, molybdenum is now 6-coordinate and the coordination polyhedron is very close to octahedral. The most notable difference between the two structures is the more closely symmetric disposition of the carbonyl ligands in $Tp^*Mo(CO)_3$.

A comparative listing of the structural parameters of $Tp^*Mo(CO)_3H$, $Tp^*Mo(CO)_3$, and $[Tp^*Mo(CO)_3]^-$ is given in Table III. The average Mo–N distances differ by no more than 0.054 Å and are all slightly longer than the mean value for pyrazolylborate complexes of molybdenum (i.e. 2.218(42) Å).[20] Mo–C distances of hundreds of structurally characterized molybdenum carbonyls average 1.978(41) Å,[20] and the distances found for the three complexes at hand closely approximate that value. The

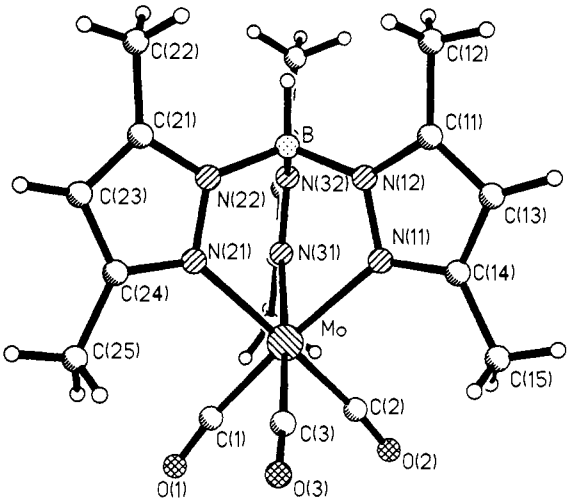

Figure 2. Molecular structure of $Tp^*Mo(CO)_3$. Interatomic distances and angles are listed in Table II.

Table III. Structural Comparison of $Tp^*Mo(CO)_3H$, $Tp^*Mo(CO)_3$, and $[Tp^*Mo(CO)_3]^-$

distance/angle	$Tp^*Mo(CO)_3H$	$Tp^*Mo(CO)_3$	$[Tp^*Mo(CO)_3]^-$
Mo–N(11)	2.252(2)	2.225(3)	2.269(5)
Mo–N(21)	2.230(2)	2.205(3)	2.260(6)
Mo–N(31)	2.230(2)	2.196(3)	2.260(6)
av	2.237	2.209	2.263
Mo–C(1)	1.977(3)	1.971(4)	1.938(7)
Mo–C(2)	1.974(3)	1.984(3)	1.940(8)
Mo–C(3)	1.987(3)	2.018(4)	1.946(8)
av	1.979	1.991	1.941
C(1)–Mo–C(2)	78.9(1)	78.4(1)	85.1(3)
C(1)–Mo–C(3)	82.1(1)	83.9(1)	85.0(3)
C(2)–Mo–C(3)	102.9(1)	93.3(1)	83.2(3)
av	na	85.2	84.4
N(11)–Mo–N(21)	85.7(1)	85.6(1)	80.3(2)
N(11)–Mo–N(31)	81.8(1)	83.0(1)	81.2(2)
N(21)–Mo–N(31)	79.8(1)	82.1(1)	82.4(2)
av	82.4	83.6	81.3
C(1)–Mo–N(21)	94.6(1)	98.4(1)	98.0(3)
C(1)–Mo–N(31)	97.3(1)	99.6(1)	94.5(3)
C(2)–Mo–N(11)	100.6(1)	97.9(1)	96.6(3)
C(2)–Mo–N(31)	90.1(1)	93.8(1)	98.3(3)
C(3)–Mo–N(11)	98.9(1)	93.9(1)	99.2(3)
C(3)–Mo–N(21)	86.9(1)	90.9(1)	96.2(3)
av	94.7	95.8	97.1

largest difference between any two average Mo–C distances is 0.050 Å. The Mo–N and Mo–C distances exhibit opposing trends, i.e. the Mo–N distances decrease in the order $[Tp^*Mo(CO)_3]^- > Tp^*Mo(CO)_3H > Tp^*Mo(CO)_3$, while the Mo–C distances in that series increase. Comparable angles of the three complexes are remarkably similar, varying by no more than 1–3°. Hence the picture that emerges is one of close similarity in structure. The latter is not too surprising, as the hydride ligand has very little steric demand and the metal orbitals whose occupation changes from compound to compound are mostly nonbonding (formally d^4–d^6). Looking ahead to the degenerate exchange reactions, one might thus expect relatively small inner-sphere reorganizational barriers for all of the processes in question, because the extent of structural change between reactants and transition state should be comparatively small. In particular, the structures of the anion ($[Tp^*Mo(CO)_3]^-$) and the radical ($Tp^*Mo(CO)_3$) are so similar, that inner-sphere reorganizational contribution to the barriers for proton and hydrogen atom transfer cannot be expected to differ significantly.

Acidities and Bond Dissociation Energies. Degenerate exchange reactions are by definition thermoneutral, and absent the "thermodynamic driving force" of a "cross reaction" there is no immediate connection between the acidity and the rate of proton

(19) Caffyn, A. J. M.; Feng, S. G.; Dierdorf, A.; Gamble, A. S.; Eldredge, P. A.; Vossen, M. R.; White, P. S.; Templeton, J. L. *Organometallics* **1991**, *10*, 2842.

(20) Orpen, G. A.; Brammer, L.; Allen, F. H.; Kennard, O.; Watson, D. G.; Taylor, R. *J. Chem. Soc., Dalton Trans.* **1989**, S1.

transfer or between the M–H bond strength and the facility of hydrogen atom transfer. However, these parameters are of interest in their own right and they may be important for design and interpretation of the experiments aimed at measuring the exchange rates.

Norton et al. have measured acid dissociation constants of various transition metal hydrides in acetonitrile;[8] Tilset and Parker have used these data in conjunction with redox potentials (measured in the same solvent) to calculate M–H bond dissociation energies (D_{M-H}).[21] In order to facilitate a meaningful comparison with these values, measurements were made in the same solvent whenever possible. However, due to the negligible solubility of $Tp^*Mo(CO)_3H$ in acetonitrile, we had to cast a slightly wider net in our attempts to determine its acidity and bond strength. Specifically, we first determined the pK_a and D_{Mo-H} for unsubstituted $TpMo(CO)_3H$. Via equilibration of $TpMo(CO)_3H$ with $Tp^*Mo(CO)_3$ the corresponding values in the Tp* system were then derived.

$TpMo(CO)_3H$ was freely soluble in acetonitrile and its pK_a could be determined by measurement of the extent of its deprotonation by aniline (eq 8):

$$TpMo(CO)_3H + PhNH_2 \rightleftharpoons TpMo(CO)_3^- + PhNH_3^+ \quad (8)$$

$$K_{eq} = \frac{[TpMo(CO)_3^-][PhNH_3^+]}{[TpMo(CO)_3H][PhNH_2]}$$

The pK_a of the anilinium ion in acetonitrile has previously been determined as 10.56.[22] This value, in conjunction with the equilibrium constant for eq 8, yields the pK_a for the metal hydride via eq 9.

$$pK_a(MH) = pK_{eq} + pK_a(PhNH_3^+) \quad (9)$$

The extent of deprotonation for three solutions containing different concentrations of $TpMo(CO)_3H$ and aniline was determined by integration of the hydride resonance versus the combined integral for the pyrazolyl protons on the Tp ligands of both the anion and hydride. Aniline catalyzed the proton transfer between $TpMo(CO)_3H$ and $[TpMo(CO)_3]^-$, resulting in coalescence of the Tp resonances. However, the hydride resonance—although slightly broadened by the exchange with the NH_2 protons—could be integrated. Three independent equilibrium measurements gave $K_{eq} = 0.186 \pm 0.057$. A pK_a of 11.3(2) for $TpMo(CO)_3H$ in acetonitrile was thus obtained.

The determination of D_{M-H} following Tilset and Parker requires knowledge of the reversible oxidation potential of the hydride's conjugate base (M^-).[21] Cyclic voltammograms of $Et_4N^+[TpMo(CO)_3]^-$ and $Et_4N^+[Tp^*Mo(CO)_3]^-$ in acetonitrile solution each exhibited a reversible oxidation wave ($Mo^{I/0}$) at moderate potentials as well as an irreversible oxidation at more positive potentials. The reversible redox processes occurred at $E^\circ = -0.53$ (for $[TpMo(CO)_3]^-$) and –0.59 V (for $[Tp^*Mo(CO)_3]^-$), while the irreversible oxidations for both compounds occurred at about +0.32 V (all potentials vs Fc^+/Fc).

With the above potentials and the pK_a value for $TpMo(CO)_3H$ in hand, its M–H bond dissociation energy can be calculated according to eq 10. This expression results from a thermochemical cycle; however, it is anchored by the known bond dissociation energy of $CpCr(CO)_3H$, which has been determined calorimetrically (D_{Cr-H} = 61.5 kcal/mol).[23]

$$D_{M-H}[\text{kcal/mol}] = 1.37pK_a + 23.06E^\circ_{ox}(M^-) + 59.5 \quad (10)$$

A value of 63(1) kcal/mol for D_{Mo-H} of $TpMo(CO)_3H$ was obtained in this manner.

Table IV. Redox Potentials, Acid Dissociation Constants, and Bond Dissociation Energies for Various Molubdenum Hydrides

compd	$E^\circ_{ox}(M^-)$ (V)[a]	pK_a[b]	D_{Mo-H} (kcal/mol)
$TpMo(CO)_3H$	–0.53	11.3	63(1)
$Tp^*Mo(CO)_3H$	–0.59	10.2	60(1)
$CpMo(CO)_3H$	–0.50	13.9	69.2
$Cp^*Mo(CO)_3H$	–0.71	17.1	68.5

[a] Reversible potential versus Fc^+/Fc for the $L_nMo/[L_nMo]^-$ couple in CH_3CN. [b] In CH_3CN.

Due to the insolubility of $Tp^*Mo(CO)_3H$ in acetonitrile, its pK_a could not be determined directly. Rather, we have determined D_{Mo-H} for $Tp^*Mo(CO)_3H$ by measurement of the equilibrium constant for the hydrogen atom transfer process of eq 11 in dichloromethane.

$$TpMo(CO)_3 + Tp^*Mo(CO)_3H \rightleftharpoons TpMo(CO)_3H + Tp^*Mo(CO)_3 \quad (11)$$

This equilibrium was rapidly established at room temperature in CD_2Cl_2 (sic!) and could be approached from either direction. However, the ^1H NMR resonances of all four species appeared sharp, i.e. the reaction is slow on the NMR time scale. Measurement of the position of equilibrium by careful integration gave K_{eq} = 153(13).

Assuming ΔS° to be negligible for this isodesmic reaction, its free energy difference ($\Delta G^\circ = -2.9(1)$ kcal) represents the difference in D_{Mo-H} between $Tp^*Mo(CO)_3H$ and $TpMo(CO)_3H$. Thus D_{Mo-H} for $Tp^*Mo(CO)_3H$ measures 60(1) kcal/mol. As bond dissociation energies are not expected to vary appreciably between different organic solvents, this number may be directly compared with those based on measurements in acetonitrile. Finally, using eq 10 in reverse, one can calculate the acid dissociation constant of $Tp^*Mo(CO)_3H$ in acetonitrile (pK_a = 10.2).

Table IV lists the redox potentials (of the $M^-/M^\bullet$ couples), pK_a's, and bond dissociation energies for both $TpMo(CO)_3H$ and $Tp^*Mo(CO)_3H$, as well as the corresponding values for the Cp and Cp* analogues for comparison.[21] The pyrazolylborate derivatives are more acidic and have noticably weaker M–H bonds. The presumed cause of both trends is the greater destabilization of the seven-coordinate hydride by the sterically more demanding Tp (or Tp*) ligand.[24] $Tp^*Mo(CO)_3H$ is one of the most acidic metal hydrides known; its bond dissociation energy is unusually low for a second-row metal—being in the range exhibited by hydrides of first-row transition metals.

Degenerate Electron Transfer. The rate of electron transfer (eq 12, in THF-d_8) was fast on the ^1H-NMR time scale over the whole temperature range investigated (–35 to +50 °C).

$$[Tp^*Mo(CO)_3]^- + Tp^*Mo(CO)_3 \rightleftharpoons Tp^*Mo(CO)_3 + [Tp^*Mo(CO)_3]^- \quad (12)$$

Mixtures of $^nBu_4N[Tp^*Mo(CO)_3]$ and $Tp^*Mo(CO)_3$ in THF-d_8 exhibited only one set of broad Tp* resonances. Rate information was obtained by analysis of the line widths according to Wahl et al.[25] This method requires information about the line widths of both the paramagnetic radical (W_p) and diamagnetic anion (W_d) in the absence of chemical exchange. Also required are the measured line widths of the samples containing both species (W_{dp}). The equation needed to relate these line widths to a second-order rate constant (k_2) is shown below (eq 13),

$$W_{dp} = f_pW_p + (1 - f_p)W_d + f_p(1 - f_p)4\pi(\Delta\nu)^2/(k_2c) \quad (13)$$

Here f_p is the mole fraction of the paramagnetic species in solution

(21) (a) Tilset, M.; Parker, V. D. *J. Am. Chem. Soc.* **1989**, *111*, 6711; correction in *J. Am. Chem. Soc.* **1990**, *112*, 2843. (b) Ryan, O. B.; Tilset, M.; Parker, V. D. *J. Am. Chem. Soc.* **1990**, *112*, 2618. (c) Parker, V. D.; Handoo, K. L.; Roness, F.; Tilset, M. *J. Am. Chem. Soc.* **1991**, *113*, 7493.
(22) Coetzee, J. F. *Prog. Phys. Org. Chem.* **1967**, *4*, 45; see also ref 8d.
(23) Kiss, G.; Zhang, K.; Mukerjee, S. L.; Hoff, C. D.; Roper, G. C. *J. Am. Chem. Soc.* **1990**, *112*, 5657.
(24) Curtis, M. D.; Shiu, K.-B. *Inorg. Chem.* **1985**, *24*, 1213.
(25) (a) Larsen, D. W.; Wahl, A. C. *J. Chem. Phys.* **1965**, *43*, 3765. (b) Chan, M.-S.; DeRoos, J. B.; Wahl, A. C. *J. Phys. Chem.* **1973**, *77*, 2163. (c) Chan, M.-S.; Wahl, A. C. *J. Phys. Chem.* **1978**, *82*, 2542. (d) Yang, E. S.; Chan, M.-S.; Wahl, A. C. *J. Phys. Chem.* **1980**, *84*, 3094.

Table V. Rate Constants for the Degenerate Electron Transfer between $Tp^*Mo(CO)_3$ and $^nBu_4N[Tp^*Mo(CO)_3]$ in THF-d_8

temp (°C)	k_2 (M^{-1} s^{-1})	temp (°C)	k_2 (M^{-1} s^{-1})
50.7	13.1×10^6	8.8	4.6×10^6
50.7	12.6×10^6	8.8	5.9×10^6
50.7	13.3×10^6	−12.6	2.4×10^6
29.9	8.9×10^6	−34.7	1.5×10^6
29.9	8.4×10^6		

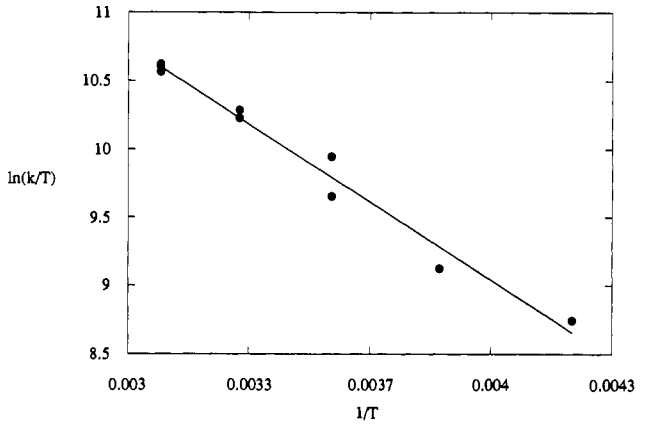

Figure 3. Eyring plot for the degenerate electron transfer (eq 12). Rate constants are listed in Table V. $\Delta H^\ddagger$ = 3.5(2) kcal/mol and $\Delta S^\ddagger$ = −15.3(6) cal/(mol·K).

($f_p = c_p/(c_p + c_d)$, c = reactant concentration). The difference in frequency between the particular Tp* resonance of $Tp^*Mo(CO)_3$ and $^nBu_4N[Tp^*Mo(CO)_3]$ is $\Delta\nu$ (in Hz). Typically f_p is 0.01–0.1, and though estimated from weights used in sample preparation, it is more accurately determined from the position of the coalesced resonance, i.e. $f_p = -(\nu_d - \nu_{obs})/(\nu_p - \nu_d)$. Equation 13 holds only for the fast exchange limit, defined as $k_2c/[2\pi(\Delta\nu)] > 3$.

Table V lists rate constants for the degenerate electron transfer at various temperatures. An Eyring plot of the data is shown in Figure 3, and the activation parameters derived therefrom were $\Delta H^\ddagger$ = 3.5(2) kcal/mol and $\Delta S^\ddagger$ = −15.3(6) cal/(mol·K). Electron transfer is very fast in this system, in accord with our expectations based on the structures of the reactants. A simple Marcus type calculation predicted an activation barrier of $\Delta G^\ddagger$ = 4 kcal/mol for this couple, to be compared to the experimental value of $\Delta G^\ddagger$ = 7.7 kcal/mol at 25 °C. Very little is known about self-exchange rates of other molybdenum complexes for comparison. The only other available data concern the $[Mo(CN)_8]^{3-/4-}$ couple ($k_2 = 3 \times 10^4$ M^{-1} s^{-1} at 25 °C in H_2O);[26] however, the large Coulombic contribution to its activation barrier and the difference in reaction media make a direct comparison of rate constants nonsensical.

Degenerate Proton Transfer. The proton transfer (eq 14, in THF-d_8) was slow on the ^1H NMR time scale, i.e. no exchange broadening of the individual resonances of $Tp^*Mo(CO)_3H$ and $^nBu_4N[Tp^*Mo(CO)_3]$ was observed up to 60 °C. However, spin

$$Tp^*Mo(CO)_3H + [Tp^*Mo(CO)_3]^- \rightleftharpoons [Tp^*Mo(CO)_3]^- + Tp^*Mo(CO)_3H \quad (14)$$

saturation transfer experiments provided evidence for chemical exchange at rates slightly below those required for coalescence.

During our initial experiments we found that irreproducibilities in the rate measurements could be traced to the presence of halide ions in the reaction solutions. Use of $^nBu_4N[Tp^*Mo(CO)_3]$ prepared by metathetical exchange of $Na[Tp^*Mo(CO)_3]$ with $^nBu_4NBr$ consistently gave higher proton transfer rates—even after repeated recrystallization—than material prepared with $^nBu_4NBF_4$. Deliberate addition of $^nBu_4NBr$ to reaction mixtures

(26) Campion, R. J.; Purdie, N.; Sutin, N. *Inorg. Chem.* **1964**, *3*, 1091.

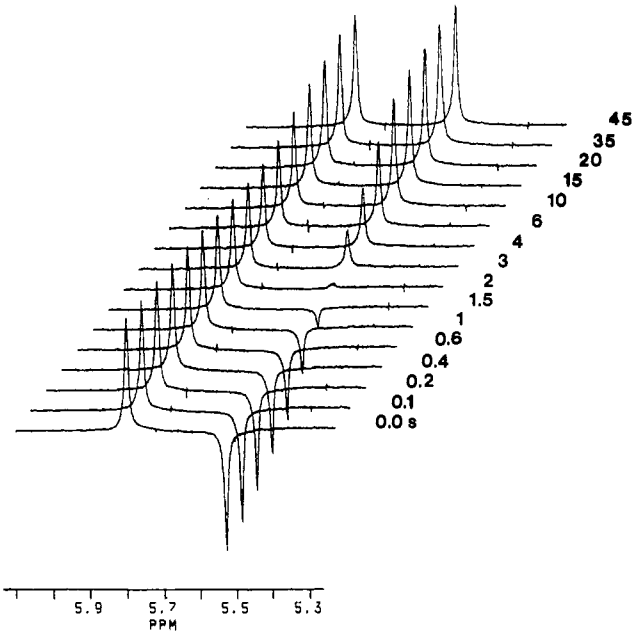

Figure 4. ^1H NMR spectra comprising one selective inversion recovery experiment for the determination of rates of degenerate proton transfer (eq 14). Spectra are labeled with delay between inversion and acquisition.

served to increase the rate of proton transfer to the point of exchange broadening the NMR resonances. Similar rate enhancements were seen upon addition of PPNCl (PPN = bis(triphenylphosphine)iminium) or Et_4NCl. The proton transfer between the metal complexes is clearly catalyzed by halide ions. These observations have precedent in both organometallic and organic[27] chemistry; note, for example, the catalysis of proton transfer between $[HMo(CO)_2(dppe)_2]^+$ (dppe = bis(diphenylphosphino)ethane) and its conjugate base by PPNCl.[28] They also inject a note of caution into the discussion of slow proton transfer rates between metal complexes. Rigorous exclusion of halides and similar small inorganic ions (e.g. OH^- from water, CN^- from nitriles etc.) from reagents and solvents is both nontrivial and clearly important for measurements of this type.

Rates of degenerate proton transfer were measured by two methods. At ambient temperature and above, the rates were measured by a selective inversion recovery NMR experiment. Having chosen a particular pair of exchanging resonances (in our case the protons in the 4-position of the pyrazole rings, as they showed the longest relaxation times), one of them was inverted selectively by a series of judiciously timed 90° pulses.[29] Thereafter the changes in intensity of both signals returning to equilibrium were monitored with time. In all cases complementary experiments were performed,[30] i.e. one in which the proton resonance of $Tp^*Mo(CO)_3H$ was inverted and another in which that of $^nBu_4N[Tp^*Mo(CO)_3]$ was inverted. Figure 4 depicts a representative series of spectra and Figure 5 shows a fit of the corresponding peak intensities with the magnetization equations. Least-squares analysis of the data was performed with the program MT-NMR and yielded the rate constants for exchange out of each site as well as the spin–lattice relaxation rates ($1/T_1$) for both sites.[30b]

Rate determinations with the inversion recovery technique were carried out in the temperature range 20–58 °C. Below 20 °C the exchange was too slow to cause measurable magnetization

(27) Emsley, J.; Gold, V.; Lee, R. A. *J. Chem. Soc., Perkin Trans.* **1986**, 1861.

(28) (a) Hanckel, J. M.; Darensbourg, M. Y. *J. Am. Chem. Soc.* **1983**, *105*, 6979. (b) Ludvig, M. M.; Darensbourg, M. Y. *Inorg. Chem.* **1986**, *25*, 2894.

(29) Robinson, G.; Kuchel, P. W.; Chapman, B. E.; Doddrell, D. M.; Irving, M. G. *J. Magn. Reson.* **1985**, *63*, 314.

(30) (a) Led, J. J.; Gesmar, H. *J. Magn. Reson.* **1982**, *49*, 444. (b) Ford, W. T.; Periyasamy, M.; Spivey, O. H.; Chandler, J. P. *J. Magn. Reson.* **1985**, *63*, 298. (c) Gesmar, H.; Led, J. J. *J. Magn. Reson.* **1986**, *68*, 95.

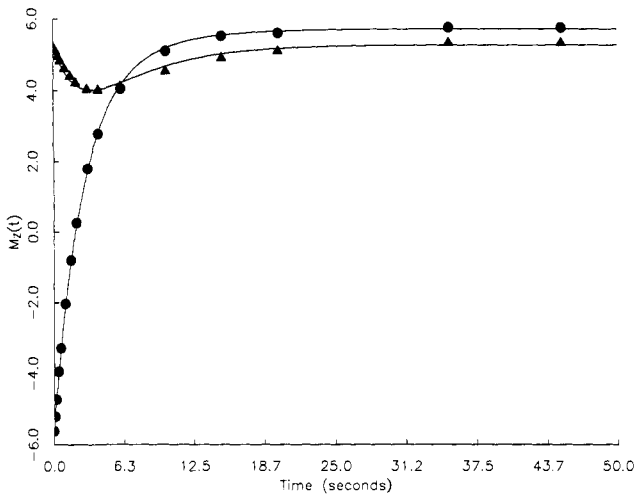

Figure 5. Plot of evolution of peak intensities (see Figure 4) with time for selective inversion recovery experiment. Lines represent fit of experimental data with the program MT NMR.

Table VI. Rate Constants for the Degenerate Proton Transfer between $Tp^*Mo(CO)_3H$ (or $(Tp^*\text{-}d_4)Mo(CO)_3H$) and $^nBu_4N[Tp^*Mo(CO)_3]$ in THF-d_8

	temp (°C)	[MoH] (M)	[Mo⁻] (M)	k_2 (M^{-1} s^{-1})
a	29.6	0.0230	0.0450	2.5
	28.7	0.0215	0.0235	3.8
	20.4	0.0218	0.0225	1.6
b	−62.5	0.0107	0.0108	0.11
	−68.6	0.0049	0.0054	0.14
	−78.2	0.0092	0.0054	0.066
	−78.2	0.0047	0.0054	0.067
	−78.2	0.0046	0.0054	0.057
	−78.2	0.0054	0.0054	0.057

[a] Selective inversion recovery experiment. [b] Isotope exchange kinetics.

transfer. Unfortunately, rates measured at temperatures above 30 °C ultimately had to be discounted too, because of an "aging" process that led to a gradual increase in the apparent proton transfer rate. This effect was noticable above 30 °C. For example, when one sample was used for consecutive rate determinations at 39.7, 49.6, 58.3, and then 29.6 °C, the last rate constant (56 M^{-1} s^{-1}) was greater than the first one (24 M^{-1} s^{-1}). Each set of complementary experiments took about 4 h; thus a slow thermal decomposition of one of the reagents may have been responsible for the rate increase. $Tp^*Mo(CO)_3H$ decomposed slowly in THF-d_8 solution above 80 °C, yielding predominantly $Tp^*Mo(CO)_3$. After 1 day at this temperature NMR detectable amounts of the radical had formed. As the electron transfer between $Tp^*Mo(CO)_3$ and $^nBu_4N[Tp^*Mo(CO)_3]$ is fast on the NMR time scale the presence of the radical in a solution $Tp^*Mo(CO)_3H$ and $^nBu_4N[Tp^*Mo(CO)_3]$ would lead to broadening of the resonances of the latter and an increase in the apparent relaxation rate. Both of these effects were noted in samples that had been heated for some time. Regardless of the exact nature of the decomposition products, only proton transfer rate constants measured below 30 °C were judged reliable and are listed in Table VI.

In order to determine activation parameters, rate measurements at different temperatures were needed. Thus we decided to follow the proton transfer by conventional kinetics at low temperature. Mixtures of $(Tp^*\text{-}d_4)Mo(CO)_3H$ and $^nBu_4N[Tp^*Mo(CO)_3]$ in THF-d_8 were prepared and their approach to equilibrium was monitored by ^1H NMR at temperatures between −60 and −80 °C. Figure 6 shows a plot of kinetic data according to the McKay equation for isotope exchange reactions (i.e. $\ln(1-F) = -Rt(a+b)/ab$).[31] Here F represents the extent of exchange at time t (i.e. $F = [Tp^*Mo(CO)_3H]/[Tp^*Mo(CO)_3H]_\infty$), R is the rate

(31) Frost, A. A.; Pearson, R. G. *Kinetics and Mechanism*, 1st ed.; John Wiley & Sons: New York, 1953; p 178.

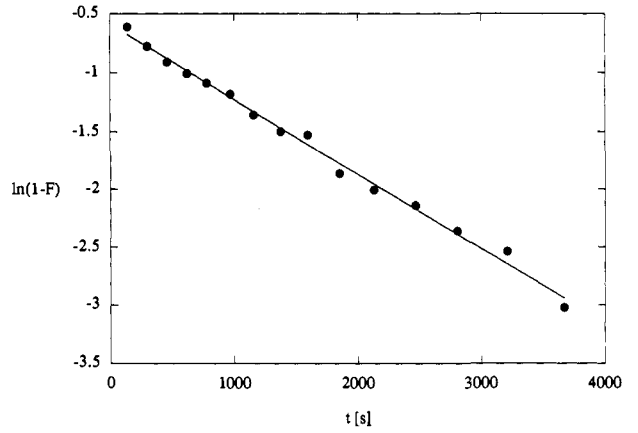

Figure 6. Plot of kinetic data for proton transfer reaction of $(Tp^*\text{-}d_4)Mo(CO)_3H$ and $^nBu_4N[Tp^*Mo(CO)_3]$ in THF-d_8 at −78.2 °C.

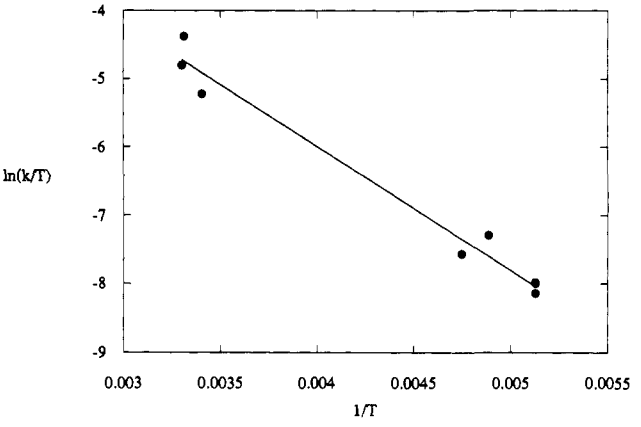

Figure 7. Eyring plot for the degenerate proton transfer (eq 14). Rate constants are listed in Table VI. $\Delta H^* = 3.6(2)$ kcal/mol and $\Delta S^* = -45(1)$ cal/(mol·K).

of exchange, and a and b are the concentrations of the two chemical species (i.e. a = [hydride] and b = [anion]). For a second-order reaction $R = k_2ab$, so that $\ln(1-F) = -k_2(a+b)t$. Plots of $\ln(1-F)$ versus time were linear for 3 half-lives or more. The resulting proton transfer rate constants are listed in Table VI also. An Eyring plot of the data spanning ca. 110 K is shown in Figure 7, and the corresponding activation parameters were $\Delta H^* = 3.6(2)$ kcal/mol and $\Delta S^* = -45(1)$ cal/(mol·K).

Rates and activation parameters for some proton self exchange reactions between metal complexes have been measured by Norton et al.[8] They have also been the subject of theoretical considerations.[3c] Our results are similar to these earlier findings, which led to the conclusion that proton transfer to metals and from metal hydrides is slow compared to that of oxygen or nitrogen acids and comparable with that of carbon acids. Most closely related to our system, the $CpMo(CO)_3H/[CpMo(CO)_3]^-$ exchange was measured at $k_2(25°C,CD_3CN) = 2.5 \times 10^3$ M^{-1} s^{-1}, $\Delta H^* = 5.3(3)$ kcal/mol, and $\Delta S^* = -25.3(12)$ cal/(mol·K). Remarkably, the major contribution to the activation barrier for the $Tp^*Mo(CO)_3H/[Tp^*Mo(CO)H]^-$ system is entropic, suggesting a highly ordered transition state.

Degenerate Hydrogen Atom Transfer. Our attempts to measure the rate of hydrogen atom transfer (eq 15) were met with several obstacles.

$$Tp^*Mo(CO)_3H + Tp^*Mo(CO)_3 \rightleftharpoons Tp^*Mo(CO)_3 + Tp^*Mo(CO)_3H \quad (15)$$

Mixtures of $Tp^*Mo(CO)_3H$ and $Tp^*Mo(CO)_3$ showed no evidence of exchange broadening in the ^1H NMR even at elevated temperatures. Early experiments involving the reaction of $(Tp^*\text{-}d_4)Mo(CO)_3H$ with $Tp^*Mo(CO)_3$ (CD_2Cl_2 solvent, monitored by ^1H NMR) were frustrated by irreproducibility; for example,

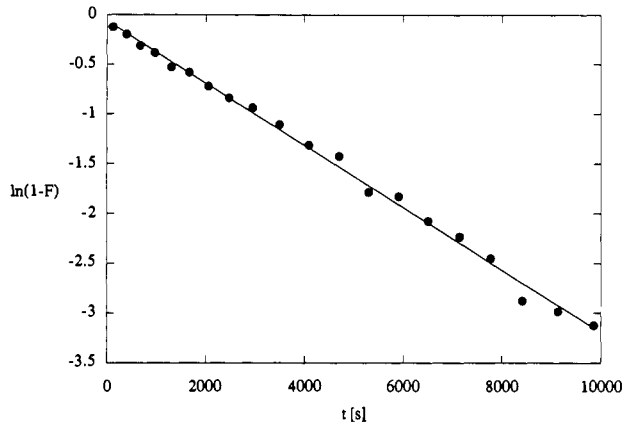

Figure 8. Plot of kinetic data for hydrogen atom transfer reaction of $Tp^*Mo(^{13}CO)_3$ and $Tp^*Mo(CO)_3H$ in THF-d_8/TsOH at −34 °C.

rate constants spanning the range 1.0 M^{-1} s^{-1} to 3.0 × 10^{-2} M^{-1} s^{-1} were measured at room temperature. Eventually it was noticed that acid washing of the NMR tubes used for the kinetics experiments tended to lower the exchange rates. Thereby alerted to the possibility of base catalysis by glass surfaces, a series of experiments was conducted in NMR tubes fitted with internal Teflon liners. However, the rate constants measured in this fashion still exhibited unacceptable variation. Finally, acid was deliberately added to the reaction mixture to protonate—and thus deactivate—any catalytic base present. A significant decrease in reaction rate was the result! The room temperature reaction of $(Tp^*\text{-}d_4)Mo(CO)_3H$ with $Tp^*Mo(CO)_3$ in CD_2Cl_2 in the presence of trichloroacetic acid yielded an apparent rate constant for hydrogen atom transfer of k_2 = 6.3 × 10^{-3} M^{-1} s^{-1}.

Recall, however, the susceptibility of the deuterium label of $(Tp^*\text{-}d_4)Mo(CO)_3H$ toward exchange with acid (see Synthesis section). The appearance of protons in the pyrazole 4-position of $Tp^*Mo(CO)_3H$ might thus reflect loss of label to the external acid rather than hydrogen atom transfer between metal complexes. Indeed, a double-labeling experiment with $(Tp^*\text{-}d_4)Mo(CO)_3H$ and $Tp^*Mo(^{13}CO)$ in CD_2Cl_2/Cl_3CCOOH (monitored by ^1H NMR) showed that loss of the deuterium label out of $(Tp^*\text{-}d_4)Mo(CO)_3H$ and incorporation into the C4-positions of $Tp^*Mo(^{13}CO)_3$ was significantly faster than formation of the product of hydrogen atom transfer, i.e. $Tp^*Mo(^{13}CO)_3H$. An upper limit of $k_2 \leq 2.0 \times 10^{-4}$ M^{-1} s^{-1} was subsequently established for the rate constant of hydrogen atom transfer in CD_2Cl_2 (at room temperature, $[Cl_3CCOOH]$ = 0.038 M).

While no appreciable solvent dependence might be expected for an atom transfer process, the direct comparison of all three degenerate transfers made use of a common reaction medium (i.e. THF) highly desirable. We found that the above the reaction mixture in THF-d_8 exhibited a transfer rate too fast to be reliably measured at ambient temperature. Eventually insufficient acid strength of trichloroacetic acid was identified as the reason for this observation. Addition of the stronger toluenesulfonic acid slowed the reaction considerably; in addition, control experiments established that the metal complexes did not react with the acid on the time scale of the kinetic measurements. For convenience in data collection the reaction temperature was lowered to −34 °C.

Reactions of $Tp^*Mo(^{13}CO)_3$ with $Tp^*Mo(CO)_3H$ in THF-d_8/TsOH were monitored by the increase in the ^{13}C NMR signal of the carbonyl resonance of $Tp^*Mo(^{13}CO)_3H$ with time. A representative plot of kinetic data for such an equilibration (using the McKay equation again) is shown in Figure 8. ^1H NMR analysis of the equilibrium mixtures revealed a C–H coupling pattern of the hydride resonance consistent with the presence of $Tp^*Mo(^{13}CO)_3H$ and $Tp^*Mo(CO)_3H$; the absence of substantial amounts of $Tp^*Mo(^{13}CO)_2(CO)H$ and $Tp^*Mo(^{13}CO)(CO)_2H$ ruled out $^{13}CO/CO$ scrambling between the complexes. Rate

Table VII. Rates of Degenerate Hydrogen Atom Exchange between $Tp^*Mo(CO)_3H$ and $Tp^*Mo(^{13}CO)_3H$ in THF-d_8 at −34 °C

[TsOH] (M)	[MoH] (M)	[Mo•] (M)	k_2 (M^{-1} s^{-1})
0.159	0.00912	0.00975	4.8 × 10^{-2}
0.100	0.00995	0.00925	2.2 × 10^{-2}
0.0592	0.00966	0.00483	2.2 × 10^{-2}
0.0592	0.00481	0.00962	1.5 × 10^{-2}
0.0583	0.00912	0.00975	1.9 × 10^{-2}
0.0583	0.00912	0.00975	1.9 × 10^{-2}
0.025	0.00995	0.00995	1.5 × 10^{-2}
0.0083	0.00995	0.00995	1.0 × 10^{-2}
0.004	0.0103	0.00916	0.9 × 10^{-2}

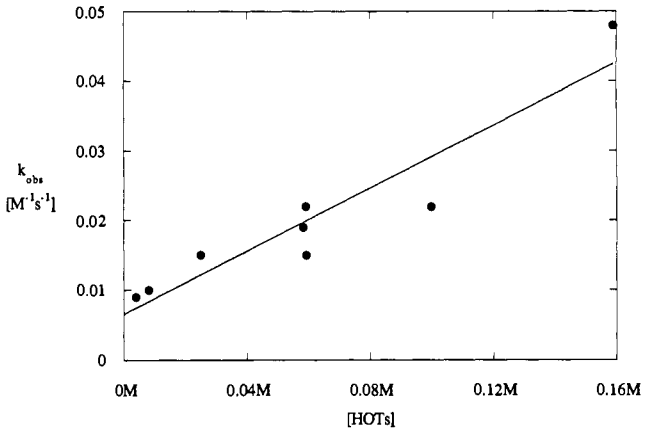

Figure 9. Dependence of rate of degenerate hydrogen atom transfer on toluenesulfonic acid concentration.

constants were reproducible. The reaction was found to be first order in both $Tp^*Mo(^{13}CO)_3$ and $Tp^*Mo(CO)_3H$. It also showed a dependence on the acid concentration. Rate constants measured at −34 °C and various acid concentrations are listed in Table VII; the same data are depicted in Figure 9.

The hydrogen atom transfer is apparently catalyzed efficiently by both bases and acids. Likely mechanisms of the catalysis are shown in Scheme I. Given the high acid strength of $Tp^*Mo(CO)_3H$ itself and the difficulty of preparing solutions free of both acids *and* bases at the same time, measurement of the intrinsic rate of uncatalyzed hydrogen atom transfer in this system may be difficult or even impossible. A simple linear extrapolation of the data in Figure 9 to zero acid concentration yielded an intercept of k_2 = 6.6 × 10^{-3} M^{-1} s^{-1}. However, in our judgement the data showed too much scatter to unambiguously establish such a linear relationship. For all the above reasons we have not attempted to determine activation parameters; their meaning would be highly ambiguous at best. Nevertheless, the slowest rate constant measured (i.e. k_2 = 9.0 × 10^{-3} M^{-1} s^{-1} at −34 °C) certainly provides an upper limit for the rate of hydrogen atom transfer. The estimated rate constant of 2 × 10^{-4} M^{-1} s^{-1} at room temperature in dichloromethane hints at the possibility of much lower intrinsic values.

We are not aware of comparable measurements of degenerate hydrogen atom transfer rates between metal complexes. However, on the basis of various observations in the literature, we find the hydrogen atom transfer studied herein remarkably slow. Most notably, Song et al.[5j] have recently reported experiments indicating a lower bound for the degenerate hydrogen atom transfer of the closely related $CpW(CO)_3H/CpW(CO)_3$ couple (eq 4) of $k_2 >$ 1 × 10^6 M^{-1} s^{-1} (in CD_3CN at 25 °C). While the corresponding electron transfer ($[CpW(CO)_3]^-/CpW(CO)_3$) is also extremely fast ($k_2 > 1 \times 10^6$ M^{-1} s^{-1}), the proton transfer ($CpW(CO)_3H/[CpW(CO)_3]^-$) is slow (k_2 = 6.5 × 10^2 M^{-1} s^{-1}), thus partially inverting the order of transfer rates observed in our system.

Conclusions. We have measured directly comparable rates of degenerate transfer reactions of electrons, protons, and hydrogen atoms between pairs of well-characterized metal complexes. At −34 °C in THF the corresponding second-order rate constants

Scheme I

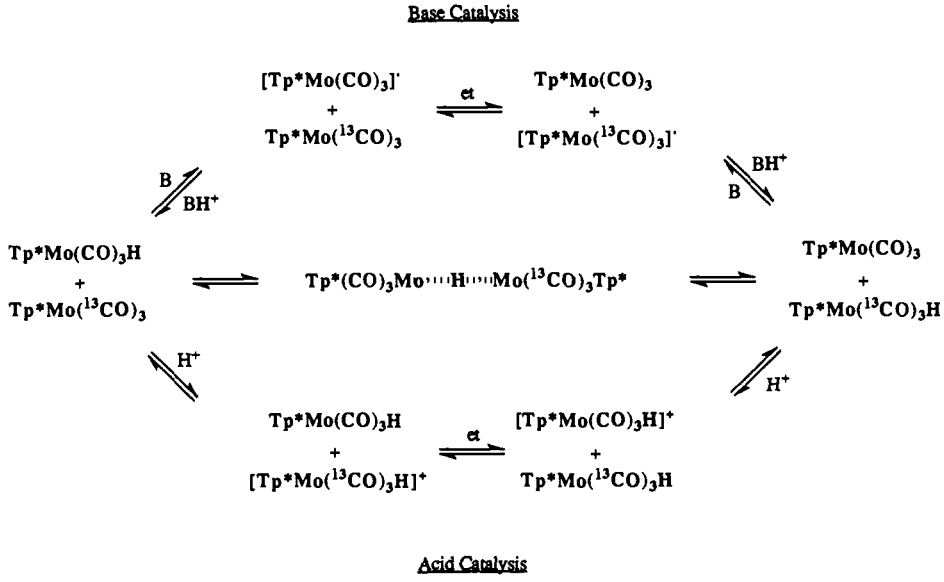

(measured or calculated using activation parameters) decrease in the order

$$k_2(e^-) = 1.4 \times 10^6\ M^{-1}\ s^{-1} > k_2(H^+) = 0.3\ M^{-1}\ s^{-1} > k_2(H^\bullet) \leq 9.0 \times 10^{-3}\ M^{-1}\ s^{-1}$$

Prior to any attempt at interpretation of the differences in rate, a critique of the meaning of these numbers is in order. How closely do the actual reactions, which proceed at these rates, correspond to the envisioned direct transfer processes? As expected, the electron transfer is very fast, and therefore probably least susceptible to catalysis. Of the two reactants, the 17-electron radical might have been expected to exhibit substitutional lability;[32] however the sluggish ^{13}CO exchange reaction proved otherwise. An inner-sphere mechanism is thus ruled out, and the quoted rate probably is an accurate measure of the facility of a simple outer-sphere electron transfer. Things are more ambiguous concerning the proton transfer. It can clearly be catalyzed. Furthermore, as "bases" like bromide ion are competent catalysts, the innocence of the THF solvent molecules might be questioned. Another possible deviation from the direct transfer path might involve an N-protonated intermediate, a structure with some precedent.[33] On the other hand, the rate of proton transfer measured by us is on the very low end of the scale reported for such reactions. Unless one is prepared to consider all of these reactions mediated by various external bases, our number gains some credence. Norton et al. have found proton transfer rates to be similar in THF and acetonitrile,[8d] thereby arguing against a special role of THF. Finally, the net hydrogen transfer observed herein in all likelihood proceeds by a combination of proton and electron transfers. However, while the intrinsic rate of the direct atom transfer remains unknown, we have established an upper limit for it. Indeed, the room temperature measurements in CD_2Cl_2 suggest that the direct hydrogen atom transfer may be too slow to significantly contribute to the net reaction under realistic chemical conditions.

The most surprising result of this study is the unexpected slowness of the hydrogen atom transfer, a process generally reputed to be very rapid. One possible explanation for this observation might be a supreme sensitivity to steric effects.[34] This notion is supported by Brown's finding of a factor of 10^4 between the rates of abstraction of hydrogen from $HSnBu_3$ by $Mn(CO)_3(P^nBu_3)_2$ and $Mn(CO)_3(P^iPr_3)_2$[35] and by our own observations in the HCo-$[P(OMe)_3]_4$/Co$[P(OMe)_3]_4$ system (see Introduction). However, the rather less dramatic effect of steric hindrance upon the proton transfer rates casts some doubt upon this rationalization. It is curious that the hydrogen atom transfer should be at least 10^8 times slower for $Tp^*Mo(CO)_3H/Tp^*Mo(CO)_3H$ than for $CpW(CO)_3H/CpW(CO)_3$, while the proton transfer rates in the corresponding couples differ by only 2 orders of magnitude.

Another possibility is, of course, that hydrogen atom transfer is inherently a slow reaction and may be masked by a facile combination of proton and electron transfers adding up to the same net reaction. While this appears to be the case in the system described herein, further studies are obviously needed to test the generality of that notion. In any case, it can no longer automatically be assumed that hydrogen atom transfer between metal complexes is fast. We hope that our results will serve as a challenge to measure hydrogen atom self-exchange rates of other hydride/radical couples.

Experimental Section

General Techniques. All manipulations of air- and water-sensitive compounds were carried out by standard Schlenk, vacuum, and drybox techniques. Pentane, diethyl ether, tetrahydrofuran, and toluene were distilled from purple Na/benzophenone ketyl solutions. Acetonitrile was distilled from P_2O_5, CH_2Cl_2 was distilled from CaH_2, and CD_2Cl_2 was distilled from P_2O_5 and stored in vacuum. THF-d_8 and benzene-d_6 were predried with potassium metal and stored under vacuum over Na/K alloy. Aniline was distilled from BaO under vacuum and stored under nitrogen at −30 °C. Acetylacetone-d_2 was prepared by stirring acetylacetone with successive portions of D_2O, followed by drying with Na_2SO_4 and distillation. ^{13}CO was purchased from Aldrich Chemical Co. (99% atom D) and stored over 3 Å molecular sieves. KTp, $Et_4N[TpMo(CO)_3]$, $Et_4N[Tp^*Mo(CO)_3]$, $TpMo(CO)_3H$, and $Tp^*Mo(CO)_3H$ were prepared according to literature procedures[11] except for the use of NaTp* instead of KTp* (we found that the former was more easily freed of all remaining pyrazole).

^1H-NMR spectra were recorded on Varian XL-400, Varian XL-200, and Bruker WM-300 spectrometers. Proton chemical shifts are referenced to residual solvent protons (benzene-d_6 7.15 ppm; THF-d_8 1.73, 3.58 ppm; CD_2Cl_2 5.32 ppm; MeCN-d_3 1.93 ppm). Probe temperatures were measured with a methanol thermometer. FTIR spectra were recorded with a Mattson Alpha Centauri FTIR spectrometer. Electrochemical measurements were performed in a drybox with use of a BAS Model CV-27 potentiostat, a Soltec Model VP-6423 X–Y recorder, a Pt disk

(32) (a) Stiegman, A. E.; Tyler, D. R. *Comments Inorg. Chem.* **1986**, *5*, 215. (b) Trogler, W. C. *Int. J. Chem. Kinet.* **1987**, *19*, 1025.

(33) Ball, R. G.; Ghosh, C. K.; nHoyano, J. K.; McMaster, A. D.; Graham, W. A. G. *J. Chem. Soc., Chem. Commun.* **1989**, 341.

(34) Eisenberg, D. C.; Lawrie, C. J. C.; Moody, A. E.; Norton, J. R. *J. Am. Chem. Soc.* **1991**, *113*, 4888.

(35) Brown, T. L. In *Organometallic Radical Processes*, Trogler, W. C., Ed.; Organomet. Chem. Library, No. 22; Elsevier: Amsterdam, 1990; pp 67–107.

working electrode, an Ag counter electrode, and a Ag/AgCl,Me_4NCl-(solvent) reference electrode. This reference electrode was made from a cracked glass bead outer shell (Fisher) which held a saturated solution of AgCl and Me_4NCl in the appropriate solvent in contact with a Ag wire. Typical substrate and supporting electrolyte ($^nBu_4BF_4$) concentrations were 1 and 100 mM, respectively. Potentials are referenced to the Cp_2Fe/Cp_2Fe^+ couple[36] (+0.68 and +0.56 V versus the Ag/AgCl(CH_2Cl_2 and MeCN) reference electrodes, respectively). Magnetic measurements were performed on a Faraday balance in the temperature range 1.7–300 K. Elemental analyses were performed by Chemical Analytical Services at the University of California at Berkeley and by Oneida Research Services Inc., Whitesboro, NY. Mass spectral analyses were performed on an AEI MS902 at the Cornell University Mass Spectrometry Facility.

NaTp*. Analogous to Trofimenko's preparation of KTp* 1.00 g of $NaBH_4$ (26.4 mmol) and 15 g of 3,5-dimethylpyrazole (156 mmol) were loaded together along with a stir bar into a 50-mL flask attached to a reflux condensor with an exit tube to monitor gas evolution (via displacement of a collum of H_2O). The reaction mixture was then slowly heated to 250 °C for an hour, evolving 3 equiv of a gas. After cooling, the mixture was crushed with mortar and pestle and placed into a sublimation apparatus. 3,5-Dimethylpyrazole was sublimed from the mixture under vacuum (10^{-4} Torr) at 100–110 °C in two batches to give a 79% yield of NaTp*. Once free of 3,5-dimethylpyrazole NaTp* was found to be completely insoluble in non-coordinating solvents like toluene, diethyl ether, or dichloromethane but freely soluble in THF or acetonitrile. NaTp* can be further purified by recrystallization from THF/Et_2O at −30 °C. Attempted purification of NaTp*-d_4 through sublimation at 280–300 °C (10^{-4} Torr) led to a significant amount of a higher molecular weight compound as evidenced by the appearance of a new peak at mass 410.0 in the mass spectrum. This compound could not successfully be separated from NaTp*-d_4 through recrystallization. NaTp*: ^1H NMR (THF-d_8) 2.08 (s, 9H), 2.28 (s, 9H), 5.50 (s, 3H) ppm; ^1H NMR (MeCN-d_3) 2.14 (broad s, 9H), 2.29 (s, 9H) 5.57 (s, 3H) ppm; ^{13}C NMR (THF-d_8) 13.38, 14.03, 103.89, 143.60, 146.59 ppm; ^{13}C NMR (MeCN-d_3) 13.29 (s), 13.82 (s), 104.36 (s), 144.30 (s), 147.84 (s) ppm; IR (Nujol) 2442 (m, ν_{BH}), 2367 (w, ν_{BH}), 1542 (m), 1435 (m), 1351 (m), 1202 (m), 1193 (m), 1175 (w), 1074 (m), 1029 (m), 817 (m), 785 (m), 731 (w), 639 (m) cm^{-1}; IR (THF) 2513 (ν_{BH}) cm^{-1}; MS 320 (M^+, base peak 225). Calcd for $NaBC_{15}N_6H_{22}$: C, 56.27; H, 6.93; N, 26.21. Found: C, 56.32; H, 6.97; N, 26.21.

NaTp*-d_4. Same preparation as above, but utilizing 3,5-dimethylpyrazole-d_2 and $NaBD_4$. MS 324 (M^+).

3,5-Dimethylpyrazole-d_2. This material was prepared via the literature procedure except that aceteylacetone-d_2 and D_2O replaced acetylacetone and H_2O.[36] Excess D_2O was used to minimize the potential loss of deuterium via exchange with unlabeled hydrazine sulfate, giving a yield of 88.3% after purification by sublimation at 100–110 °C (10^{-4} Torr). By ^1H NMR it was estimated that the deuterium incorporation at the C-4 position was approximately 95%. ^2H NMR showed less than 1% deuterium incorporation at the methyl positions, in agreement with the mass spectrum of the material.

Tp*Mo(CO)$_3$. Oxidation of $Et_4N^+[Tp^*Mo(CO)_3]^-$ with Cp_2FePF_6 in MeCN following the procedure of Shiu and Lee[13] was found to give near quantitative yields of $Tp^*Mo(CO)_3$. The product was further purified by recrystallization from CH_2Cl_2/Et_2O at −30 °C. IR(toluene) ν_{CO} 1997 (s, sharp), 1860 cm^{-1} (s, broad); IR (Nujol) ν_{CO} 1992 (s, sharp), 1836 (s, broad) cm^{-1}; IR (KBr) ν_{CO} 1997 (s, sharp), 1851 (s, broad) cm^{-1}. Calcd for $MoBC_{18}H_{22}N_6O_3$: C, 45.31; H, 4.65; N, 17.61. Found: C, 44.99; H, 4.65; N, 17.36.

Tp*Mo(^{13}CO)$_3$. $Tp^*Mo(CO)_3$ (0.514 g, 1.1 mmol) in 40 mL of THF was freeze–pumped thawed two times on a high-vacuum line and 480 Torr of ^{13}CO was introduced (2.5 mmol). After the mixture was stirred at room temperature overnight there was no detectable ^{13}CO incorporation by IR. Repeating the above procedure on the same sample at 80 °C did not yield any labeled product either. The THF was stripped off, and the radical was dissolved in 150 mL of toluene and exposed to 190 Torr of ^{13}CO (3.6 mmol) at 110–110 °C. After 2 days at this temperature ^{13}CO incorporation could be easily seen by IR. This process was repeated three times more to yield $Tp^*Mo(^{13}CO)_3$ with a 93.6% total ^{13}CO incorporation, judged to be 82% trisubstituted, 16% disubstituted, and ≤2% monosubstituted by ^1H NMR on a sample of $Tp^*Mo(^{13}CO)_3H$ prepared from this complex by reduction with Na in THF and subsequent protonation with $ClCH_2COOH$ ($Tp^*Mo(^{13}CO)_3H$: IR(KBr) ν_{CO} 1952, (s, sharp), 1861, 1837 (s, broad) cm^{-1}; ^1H NMR (CD_2Cl_2) 3.41 (q, 1H, $^2J_{CH}$ = 11 Hz) ppm, contaminated with $Tp^*Mo(^{13}CO)_2(CO)$, 3.41 (t, 1H, $^2J_{CH}$ = 11 Hz) ppm). No evidence for decomposition of $Tp^*Mo(CO)_3$ was seen at these temperatures. IR (KBr) ν_{CO} 1950 (s, sharp), 1811 (s, broad); IR (Nujol) ν_{CO} 1947 (s, sharp), 1793 (s, broad) cm^{-1}.

^{n}Bu$_4$N[Tp*Mo(CO)$_3$]. NaTp* (1.00 g, 3.1 mmol) and 0.82 g of $Mo(CO)_6$ (1.0 equiv) were heated to reflux in 20 mL of MeCN under argon for 8 h. The solution was degassed and then taken into a drybox where 1.06 g of $^nBu_4NBF_4$ was added to the yellow solution. This solution was stirred for 15 min followed by filtration to remove a white precipitate. The MeCN was removed under vacuum and the remaining yellow solid triturated twice with CH_2Cl_2. The solid was dissolved in CH_2Cl_2/Et_2O and cooled to −30 °C. Clear crystals developed and were filtered from their mother liquor. Upon washing with Et_2O these turned to a fine white powder and after drying gave 1.61 g of $^nBu_4N[Tp^*Mo(CO)_3]$ (72%). ^1H NMR (THF-d_8) 1.02 (t, 12H), 1.46 (m, 8H), 1.75 (s, 8H), 2.29 (s, 9H), 2.48 (s, 9H), 3.35 (m, 8H), 5.57 (s, 3H) ppm; ^1H NMR (MeCN-d_3) 0.96 (t, 12H), 1.33 (m, 8H), 1.59 (m, 8H), 2.32 (s, 9H), 2.44 (s, 9H), 3.07 (m, 8H), 5.69 (s, 3H) ppm; IR (KBr) 2961 (m), 2948 (m), 2874 (m), 2518 (w, ν_{BH}), 1882 (s, ν_{CO}), 1728 (s, ν_{CO}), 1542 (m), 1483 (w), 1445 (w), 1414 (m), 1382 (m), 1203 (m), 1065 (w), 1043 (w), 811 (w), 771 (w) cm^{-1}; IR (CH_2Cl_2) ν_{CO} 1883, 1743 cm^{-1}; IR (MeCN) ν_{CO} 1886, 1749 cm^{-1}; IR (toluene) ν_{CO} 1878, 1738 cm^{-1}.

Crystal Structure of Tp*Mo(CO)$_3$H. A suitable crystal was grown by pentane vapor diffusion into a saturated solution of $Tp^*Mo(CO)_3H$ in CH_2Cl_2. Crystals tended to grow in prisms having one long axis, so a crystal with dimensions ~0.9 × 0.3 × 0.2 mm was cut with a razor blade to ~0.3 × 0.3 × 0.2 mm. The crystal was then mounted in a 0.5-mm capillary tube with grease to hold it in place. Data collection was carried out at −75 °C. Crystal data and data collection parameters are listed in Table VIII. Positional and thermal parameters are included in the supplementary material.

Crystal Structure of Tp*Mo(CO)$_3$. A suitable crystal was grown by pentane vapor diffusion into a saturated CH_2Cl_2 solution of $Tp^*Mo(CO)_3$. The crystal was mounted on the tip of a pulled glass fiber with epoxy glue to hold it in place. Data collection was run at −75 °C to facilitate comparisons to the previously determined structure of $Tp^*Mo(CO)_3H$. Crystal data and data collection parameters are listed in Table

Table VIII. Crystal Data and Data Collection Parameters for $Tp^*Mo(CO)_3H$ and $Tp^*Mo(CO)_3$

	$Tp^*Mo(CO)_3H$	$Tp^*Mo(CO)_3$
formula	$C_{18}H_{23}BN_6O_3Mo$	$C_{18}H_{22}BN_6O_3Mo$
color, habit	yellow rectangular prisms	red rectangular prisms
crystal size (mm)	0.3 × 0.3 × 0.2	0.1 × 0.2 × 0.3
crystal system	monoclinic	monoclinic
space group	$P2_1/c$	$P2_1/c$
unit cell dimens		
a (Å)	8.005(3)	7.962(4)
b (Å)	13.873(5)	13.885(6)
c (Å)	18.874(5)	19.048(5)
β (deg)	97.73(2)	96.86(2)
volume, Å^3	2077.2(12)	2090.7(14)
Z	4	4
formula wt	478.2	477.2
density(calcd) (g/cm^3)	1.529	1.516
abs coeff (mm^{-1})	0.645	0.641
diffratometer	Siemens R3m/V	Siemens R3m/V
radiation	Mo Kα (λ = 0.71073 Å)	Mo Kα (λ = 0.71073 Å)
temp (K)	198	198
2θ range (deg)	0.0–55.0	0.0–50.0
scan type	2θ–θ	2θ–θ
scan range	1.20° plus Kα separation	1.00° plus Kα separation
no. of reflcns	4157	4173
no. of independent reflcns	3689	3708
no. of obsd reflcns	3401 (F > 3.0σ(F))	3261 (F > 3.0σ(F))
system	SHELXTL PLUS	SHELXTL PLUS
solution	direct methods	direct methods
refinement	full-matrix least-squares	full-matrix least-squares
R (%)	3.00	3.24
Rw (%)	4.42	3.39
GOF	1.76	2.21
data-to-parameter ratio	13.0:1	12.4:1

(36) Gagne, R. R.; Koval, C. A.; Lisensky, G. C. *Inorg. Chem.* **1980**, *19*, 2855.

(37) Rabjohn, N., Ed., *Organic Syntheses*; John Wiley & Sons: New York: 1963; Vol. 4, p 351.

VIII. Positional and thermal parameters are included in the supplementary material.

Determination of the pK_a of $TpMo(CO)_3H$. The extent of equilibrium deprotonation of $TpMo(CO)_3H$ by aniline in acetonitrile-d_3 was determined by ^1H NMR. A stock solution of $TpMo(CO)_3H$ in MeCN-d_3 (24.5 mg in 2.0 mL) was prepared in the drybox. Four NMR tubes were charged with 0.5 mL each of this solution. Into three of the samples was injected 1, 2, and 3 μL of aniline, respectively, and the tubes were sealed with septa. The ^1H NMR integral of the combined pyrazole protons of the hydride and anion (brought into the fast exchange by aniline) versus that of the molybdenum hydride resonance yielded values for the relative concentrations for all four species in eq 8. The mean value for K_{eq} was 0.186 ± 0.057 ($K_{eq} = 0.174$, 0.135, and 0.248 for the three individual experiments).

Selective Inversion Recovery Experiments. The basic experiment is described in the text. Prior to each run the 90° pulse width was calibrated by a determination of the 180° pulse length (null condition). The entire pulse sequence was carried out by a program written for use on a WM-300 Bruker instrument. Each spectrum resulted from 8 scans with a relaxation delay of at least 5–6 T_1's of the pyrazol ring protons of the hydride complex (typical T_1 at room temperature on a freshly prepared sample was 7–8 s); 45–60-s delays were used. All experiments used at least 16 spectra to sample the return to equilibrium. Spectra were accumulated in the absolute intensity mode. Samples were not spun during acquisition to avoid magnetization transfer via spinning sidebands.[38] Temperatures were measured after each experiment with a methanol thermometer.

Data analysis involving biexponential fitting of only the inverted site's return to equilibrium was performed on the Cornell University Hewlett Packard departmental computer using the nonlinear regression capabilities of the program PLOT. As stated by Led and Gesmar,[30] rates below ~ 10 M^{-1} s^{-1} ($\lambda_1/\lambda_2 \leq 4$) using the concentrations and temperatures available yielded curves which were equally well fit with either an exponential or a biexponential expression, and thus required a full mathematical analysis of all four magnetization curves of both the normal and complementary experiment.

Full data analysis was performed by the program MT-NMR, an ANSI standard FORTRAN program developed by Spivey and co-workers (obtained from Dr. O. Spivey, Oklahoma State University)[30b] and run on the Cornell Chemistry Department Hewlett Packard computer. This program can minimize all 11 parameters (R_{1A}, R_{1B}, k_A, k_B, $M_{\infty A}$, M_{0A}, $M_{\infty B}$, M_{0B}, $^*M_{0A}$, $^*M_{0B}$, and α) or any lesser number with others remaining at fixed values. The ratio of the line widths, α, was determined from the equilibrium intensities of the anion and hydride pyrazole protons and a knowledge of the concentrations of the respective species. This value was always very close to one ($\sim$0.9 to 1.1) and was held fixed. The exchange rate from site B, k_B, was defined by the expression $k_B \approx \alpha k_A M_{A\infty}/M_{\infty B}$. During the first round of the fitting procedure R_{1A} was held constant and then allowed to float in a second fitting. The first round thus minimized 8 parameters, and the second fit 9 parameters. The initial estimates of the initial and final magnetizations could be made fairly well from the data, and MT-NMR returned reasonable values for these as judged by the plots of $M_z(t)$ versus time. The returned relaxation rate constants were always within the expected ranges for T_1's determined on samples containing the respective species. The estimates of the error in the rate constants from this procedure were much smaller than the scatter between experiments.

Low-Temperature H^+ and $H^\bullet$ Transfer Studies. Stock solutions of the required two complexes were prepared in the drybox using standard volumetric and syringe techniques. The compounds used were very oxygen sensitive in solution, so a "double septum" technique was developed. This involved first sealing an NMR tube with a plug of rubber (a septum that was trimmed of most of its top portion) inserted about 10 mm into the NMR tube, which was followed by capping with a septum and wrapping with parafilm. Samples prepared in this way showed no evidence of oxygen contamination during the kinetic measurements. Spectra were recorded at desired time intervals by a program written for the Bruker instrument. A typical experiment was run by first chilling a sample of one of the reactants to the desired temperature in the probe of the NMR spectrometer. The sample was then ejected, a concentrated solution of the other reactant at room temperature was quickly injected into the tube, the tube was dropped back into the probe, and acquisition was started. Since the hydride complex appeared to be the most thermally sensitive, it was always the reagent chilled in the NMR tube prior to injection of the radical or anion. To obtain infinity values in each experiment, samples were ejected from the chilled probe, warmed to room temperature, dropped back in, and allowed to equilibrate; three spectra were then recorded to give a mean infinity value.

The proton transfer reactions were studied by ^1H NMR, and relaxation delays of at least $5T_1$ were used. At lower temperatures the T_1's for both the hydride and anion pyrazole sites decreased from 7 and 3 to $\leq$2 s for both, thus a relaxation delay of 10 s was used. The McKay equation was used to interpret kinetic data.[31]

The hydrogen atom transfer studies relied upon ^{13}C peak intensities of $Tp^*Mo(^{13}CO)_3H$. The T_1 for this resonance at room temperature at −34 °C was about 3 s. In order to maximize signal to noise in these experiments, calculated Ernst angles for the pulses were used, based on the estimated value of T_1 and a 90° pulse width. The reliability of this technique was checked in several cases by using a sealed capillary of THF-d_8/$CHBr_3$ (1:3 by volume) in the same tube as a peak intensity standard. The T_1 of the carbon in neat $CHBr_3$ is 1.65 s,[39] and it was found to be very close to the T_1 of $Tp^*Mo(CO)_3H$ in the THF-d_8/$CHBr_3$ mixture at −34 °C. Rates were the same with or without scaling of peak heights to this standard. Peak intensity data were analyzed with the McKay equation. It was also found that more consistent results for the atom transfer could be realized by first chilling the solution of the hydride in dry ice/acetone, followed by injection of the radical solution and insertion of the sample into the probe at −34 °C.

Electron Self-Exchange Reaction. $^nBu_4N[Tp^*Mo(CO)_3]$ (21.7 mg) and 2 μL of hexamethyldisiloxane were combined with 0.6 mL of THF-d_8 into an NMR tube. Another tube was prepared containing 9.8 mg of $Tp^*Mo(CO)_3$ and 2 μL of hexamethyldisiloxane. A third tube contained 21.6 mg of $^nBu_4N[Tp^*Mo(CO)_3]$, 2 μL of hexamethyldisiloxane, and 2.2 mg of $Tp^*Mo(CO)_3$ in 0.6 mL of THF-d_8. All three tubes were brought out of the drybox and flame sealed under N_2. Spectra were recorded at the temperatures listed in Table V. Line widths were determined by either measurement of the line width at half-height by hand from plotted spectra or fitting the spectra with lorentzian line shapes generated by the software available on the Bruker instrument. Corrections to all line widths for field inhomogeneity broadening were made by subtraction of the line width of hexamethyldisiloxane in each sample (ca. 1 Hz). Corrections were also applied for the expansion and contraction of THF over this temperature range.

Acknowledgment. We thank Prof. H. O. Spivey (Oklahoma State University) for sending us a copy of the program MT NMR. Acknowledgment is made to the donors of the Petroleum Research Fund, administered by the American Chemical Society, for partial support of this research, and to NSF for a Presidential Young Investigator Award to K.H.T.

Supplementary Material Available: IR spectra of $Tp^*Mo(CO)_3H$ and $Tp^*Mo(CO)_3D$ and tables of X-ray structure determinations of $Tp^*Mo(CO)_3H$ and $Tp^*Mo(CO)_3H$, including atomic coordinates, anisotropic thermal parameters, and hydrogen atom positions (10 pages). Ordering information is given on any current masthead page.

(38) Curzon, E. H.; Howarth, O. W. *J. Chem. Soc., Chem. Commun.* **1984**, 1012.

(39) Farrar, T. C.; Druck, S. J.; Shoup, R. R.; Becker, E. D. *J. Am. Chem. Soc.* **1972**, *94*, 699.